GAMMA-GAMMA DIRECTIONAL CORRELATION STUDIES IN STRONGLY DEFORMED NUCLEI

A Dissertation

Presented to

the Faculty of the Graduate School

University of Manitoba

In Partial Fulfilment

of the Requirements for the Degree

Doctor of Philosophy

by

R. C. Williams

August, 1956

TABLE OF CONTENTS

		Page
List of Plates and Figures		iii
Abstract		v
CHAPTER I.	THEORETICAL CONSIDERATIONS	1
	a) Introduction	1
	b) Theory of Gamma-Gamma Directional Correlation	3
	c) The Collective Model of the Nucleus	20
	d) The Treatment of Experimental Data	25
CHAPTER II.	COINCIDENCE METHOD	32
	a) Coincidence Spectrometry	32
	b) The Apparatus	37
	c) Calibration of the Spectrometer	51
CHAPTER III.	EXPERIMENTAL RESULTS	56
	a) Application of the Fast-Slow Coincidence Spectrometer to Ni^{60}	56
	b) Directional Correlation in W^{182}	61
	(i) Properties of W^{182}	61
	(ii) Procedure	65
	(iii) Spin and Multipolarity Assignments	66

Page

c) Directional Correlation in Sm^{152}..... 84

(i) Properties of Sm^{152}..... 84

(ii) Procedure..... 88

(iii) Spin and Multipolarity Assignments... 88

d) Directional Correlation in Ta^{181}..... 92

(i) Properties of Ta^{181}..... 92

(ii) Procedure..... 96

(iii) Spin and Multipolarity Assignments... 98

CHAPTER IV. SUMMARY AND CONCLUSIONS..... 104

ACKNOWLEDGEMENTS..... 108

REFERENCES..... 109

LIST OF PLATES AND FIGURES

Page

PLATES

1. The Three Channel Coincidence Spectrometer..... 38
2. The Photomultipliers and the Source..... 40

FIGURES

1. Geometry of the detecting system..... 29
2. The 6BN6 coincidence circuit..... 45
3. The Fast-Slow coincidence circuit..... 47
4. Arrangement for angular resolution measurements using collimated beam..... 53
5. (a) Angular resolution curve for the 67.4 photoelectron line in W^{182}..... 55
5. (b) Angular resolution curve for the 1172 kev line in Ni^{60}..... 55
6. Decay scheme of Co^{60}..... 60
7. Directional correlation function for Ni^{60}..... 62
8. Energy levels in W^{182}..... 64
9. Gamma ray spectrum of Ta^{182}..... 67
10. Directional correlation for the 67.4 → 1222 kev cascade in W^{182}..... 71
11. Directional correlation for the 152.4 → 1122 kev cascade in W^{182}..... 75
12. Directional correlation for the 67.4 → 1122 kev cascade in W^{182}..... 78

Page

13. Plot of A versus δ..... 80

14. Level scheme of W^{182} as predicted by the collective model of the nucleus..... 82

15. Gamma ray spectrum of $Eu^{152,154}$..... 85

16. Decay scheme of Eu^{152}..... 86

17. Directional correlation for the 244 → 122 kev cascade in Sm^{152}..... 91

18. Gamma ray spectrum of Hf^{181}..... 93

19. Decay scheme of Ta^{181}..... 94

20. Directional correlation for the 132 → 345 kev cascade in Ta^{181}..... 100

21. Level scheme of Ta^{181} as predicted by the collective model of the nucleus..... 102

ABSTRACT

A fast-slow coincidence spectrometer has been developed to operate at a resolving time of 2×10^{-8} seconds. This spectrometer was calibrated with the 1172 → 1332 kev cascade in Ni^{60}.

The isotopes $_{72}W^{182}$, $_{62}Sm^{152}$ and $_{73}Ta^{181}$ were studied because they provided a test for the theory of the collective model of the nucleus. These isotopes have many nucleons outside of closed shells resulting in large nuclear deformations, hence they are called "strongly deformed nuclei."

The 67.4 → 1222 kev cascade in W^{182} gave a correlation which satisfies a 2 → 2 → 0 assignment, the 67.4 kev transition being pure E_1 and the 1222 kev transition being pure E_2.

The 152.4 → 1222 kev cascade in W^{182} gave a correlation which satisfies a 3 → 2 → 0 assignment. The 152.4 kev transition is pure E_1.

The 67.4 → 1122 kev cascade in W^{182} was shown to have the assignment:

$2(E_1) \rightarrow 2(90\%\ E_2,\ 10\%\ M_1) \rightarrow 2$. These results verify the prediction of the collective model based on the existence of K-forbiddenness in W^{182}.

The 244 → 122 kev cascade was studied in Sm^{152}, with the resulting assignment

$$4(E_2) \rightarrow 2(E_2) \rightarrow 0$$

The 132 → 345 kev cascade was studied in Ta^{181} with the resulting spin assignments

$$1/2(E_2) \rightarrow 5/2(E_2) \rightarrow 9/2.$$

These two assignments also agree with the predictions of the collective model.

Chapter I

Theoretical Considerations

(a) Introduction

The scintillation counter, since its conception as a device by Kallman (1) has been the basis of gamma-ray spectroscopy. Brady and Deutsch (2) incorporated it as a means of studying the spin assignments of the energy levels of gamma-emitting nuclei by performing angular correlation experiments based on the pioneer work of Hamilton (3) on the theory of directional correlation. The problem in directional angular correlation is as follows: a nucleus emits two gamma-rays g_1 and g_2 consecutively with less than a microsecond between their emission times. One then asks what is the relative probability $W(\theta)d\Omega$ that g_2 is emitted into a solid angle $d\Omega$ at an angle θ with respect to g_1. Hamilton was the first to work out the theoretical expression for the correlation function $W(\theta)$ for a large number of cases of interest.

Experimentally one counts the number of coincidences between g_1 and g_2 as a function of the angle subtended by the axes of the two counters. Comparison of the experimental correlation function with theory provides the desired information about the properties of the nuclear levels and the radiations. The complete specification of the correlation function requires five parameters: The multipole orders L_1 and L_2 of the gamma-rays g_1 and g_2 and the spins j_1, j and j_2 of the initial,

intermediate and final nuclear states. Thus the directional correlation measurement alone never allows a complete determination of all nuclear parameters involved. Only in conjunction with other methods is it possible to establish a complete decay scheme. The parities of the nuclear states cannot be determined in a directional correlation experiment, and the fact that the correlation function $W(\theta)$ does not depend on the parities of the nuclear states can be understood classically. Electric and magnetic radiations of the same multipole orders L are related by the transformation $\underline{E} \rightarrow \underline{H}$, $\underline{H} \rightarrow -\underline{E}$. This transformation leaves the Poynting vector and therefore the angular distribution of the radiation unaltered. Thus it is impossible to distinguish between electric and magnetic radiation by means of a directional correlation experiment. They can be distinguished, however, by a polarization-direction correlation experiment.

This thesis is concerned with gamma-gamma directional correlation experiments on four different radio-isotopes. Chapter I summarizes the theory needed to understand the physics of angular correlation. Chapter II is concerned with the electronic details of coincidence spectrometry and the calibration and corrections used on such equipment. Chapter III describes and analyzes the results of the measurements on the four isotopes. It is found that the results can be described by the collective model of the nucleus. Chapter IV is a summary of this work along with its conclusions.

(b) Theory of Gamma-Gamma Directional Correlation

The theory of gamma-gamma directional correlation has been treated from the point of view of standard perturbation methods (3) and group theoretic techniques (4). The perturbation methods enable one to derive some physical insight into the processes involved hence this section will give a brief exposition of these techniques. Biedenharn and Rose's review article (4) on the theory contains some results which will simply be stated at the end of this section.

Consider a nucleus which is initially in an excited state A and undergoes two successive emissions of quanta, thus passing through an intermediate state B and ending in a final state C. Let the total angular momentum of the initial, intermediate and final states be $\underline{J}_1$, $\underline{J}$ and $\underline{J}_2$ with eigenvalues $\sqrt{j_1(j_1+1)\hbar^2}$, $\sqrt{j(j+1)\hbar^2}$ and $\sqrt{j_2(j_2+1)\hbar^2}$; J_{1z}, J_z and J_{2z} are their z components with eigenvalues $m_1\hbar$, $m\hbar$ and $m_2\hbar$. The m-states of each level total $(2j+1)$ in number.

It was pointed out in the introduction that a correlation does exist between the direction of emission of the second quanta relative to the first. One then asks what is the probability that the second quantum will be emitted at an angle θ relative to the first? This probability function represents the correlation between the two directions of emission.

The calculation starts with the Hamiltonian of the system, in particular with the interaction term which is really

the coupling between the nucleons and the radiation field. This interaction term causes the transitions with which we are concerned hence we shall devote a few lines to it.

The individual nucleons in the nucleus are charged particles that see a vector potential $\underline{A}$ due to the radiation field (the quanta under consideration). If one assumes that the velocities of the nucleons are non-relativistic then the interaction between the nucleons and the quanta is:

$$H = -\int \underline{i} \cdot \underline{A}\, dv = -\frac{1}{c}\int \rho\, \dot{\underline{r}} \cdot \underline{A}\, dv \qquad (1.1)$$

where $\underline{i}$ and ρ are the current and charge densities of the nucleons involved in the transition.

The vector potential can be represented by plane waves of amplitude q, polarization $\underline{e}$ and wave number $\underline{K} = k\underline{K}_o = 2\pi\nu c^{-1}\, \underline{K}_o$. $\underline{K}_o$ is the propagation direction and ν is the frequency. Hence

$$\underline{A} = q\, \underline{e}\, \exp(i\, \underline{K}\cdot\underline{r}). \qquad (1.2)$$

The amplitude q is a function of time but independent of position. The interaction between the nucleons and the quanta thus become

$$H(\underline{K}_o, \underline{e}) = -\frac{q}{c}\, \underline{e} \cdot \int \rho\, \underline{r}\, e^{i\underline{K}\cdot\underline{r}}\, dv. \qquad (1.3)$$

The exponential in the integrand is now expanded in a Taylor series. One takes cognizance of the fact that the multipole moments of a system with charge and current densities ρ and $\underline{i}$ are given by:

$$\underline{P} = \int \rho \, \underline{r} \, dv = \text{electric dipole moment.} \qquad (1.4)$$

$$\underline{Q} = \int \rho \, \underline{rr} \, dv = \text{electric quadrupole moment.} \qquad (1.5)$$

$$\underline{M} = \frac{1}{2} \int \underline{r} \times \underline{i} \, dv = \text{magnetic dipole moment.} \qquad (1.6)$$

Suitable re-arrangements of the terms in the series expansion of $\exp(i\underline{K} \cdot \underline{r})$ along with the above definitions leads to:

$$H(\underline{K}_o, \underline{e}) \cong \underline{e} \cdot (\underline{P} + \underline{M} \times \underline{K}_o + i\pi\nu c^{-1} \, \underline{Q} \cdot \underline{K}_o + \ldots). \qquad (1.7)$$

This is the result when the interaction term is expanded in terms of the multipole moments of the system. When the radiation observed is caused by any one of these terms the radiation has the same multipolarity as the perturbing term, i.e. the radiation will be electric dipole, electric quadrupole or magnetic dipole, etc. depending upon whether it was caused by $\underline{P}$, $\underline{Q}$ or $\underline{M}$, etc. Since we are dealing with a linear system with each term in the multipole expansion of $H(\underline{K}_o, \underline{e})$ independent of the other, the transitions between the different levels can have different multipole characteristics. That is to say, the electric dipole term can cause the transition from A $\rightarrow$ B while the electric quadrupole term can cause the transition from B $\rightarrow$ C. Thus the first gamma-ray would be electric dipole in character while the second would be electric quadrupole.

The matrix elements that enter into the calculation of the directional correlation function will be precisely the matrix elements of the multipole moments of equation (1.7).

Since the radiation field has been represented by plane waves it can be quantized by quantizing the amplitudes of these plane waves. This quantization leads to the well known representation of the radiation field by an assembly of simple harmonic oscillators. These oscillators have certain occupation numbers that are related to the amplitudes of the plane waves chosen to represent the radiation field.

Because of these occupation numbers all the states of the system (nucleus plus radiation field) can be specified. The states of the nucleus are specified by the number of m-states in each level while the radiation field is specified by the occupation numbers. The states of the nucleus will be designated as A_ℓ, B_n and C_p where the subscripts are values of m. The occupation numbers of the field oscillators will be n_i.

Thus the initial state can be represented by the numbers $(A_\ell, n_1 \ldots n_\rho \ldots n_\sigma \ldots)$ and quantum mechanically the probability of finding the system in that state will be given by the square of the absolute value of the probability amplitude a_i. The system emits a photon, thereby undergoing a transition where the nucleus is now in an intermediate state B_n and the occupation number of the field oscillator which has accepted the photon will have increased by one. If this photon is emitted into the ρ-th field oscillator the intermediate state can be specified by the numbers

$(B_n, n_1 \ldots n_\rho + 1 \ldots n_\sigma \ldots)$ with an associated probability amplitude $b_{n\rho}$. The subscript ρ on the b indicates an increase in the number of entities in the system.

The system now emits a second photon into the σ-th field oscillator. The nucleus has thus passed to the final state specified by C_p and the occupation number of the σ-th field oscillator increases by one due to the photon it has accepted. The final state is thus specified by the numbers $(C_p, n_1 \ldots n_\rho + 1 \ldots n_\sigma + 1 \ldots)$ with an associated probability amplitude $c_{p\rho\sigma}$. The square of the absolute value of this probability amplitude will thus yield the probability of finding the system with the nucleus in the final state C_p and the occupation numbers of the ρ-th and σ-th field oscillators increased by one indicating the emission of two photons.

One finds $c_{p\rho\sigma}$ by solving the equation

$$-i \hbar \dot{a}_j = \sum_k H_{jk} a_k + E_j a_j \qquad (1.8)$$

which governs the time dependence of the probability amplitudes a_j and a_k. The a_j and a_k refer to any of the above a_ℓ, $b_{n\rho}$ or $c_{p\rho\sigma}$. H_{jk} is the matrix element due to the interaction (1.3). Hamilton (3) in particular writes down three equations that connect a_ℓ, $b_{n\rho}$ and $c_{p\rho\sigma}$. Specification of $a_\ell(t=0)$ constitutes a statement of the initial conditions. Certain solutions to these three equations are assumed which enable the probability amplitudes to be calculated.

It turns out that these probability amplitudes depend on the product of two factors. The first factor depends on the time t, ν_ρ, ν_σ, $\gamma(A_\ell)$ and $\gamma(B_n)$. The quantities ν_ρ and ν_σ are the frequencies associated with the ρ-th and σ-th field oscillators while $4\pi\gamma(A_\ell)$ and $4\pi\gamma(B_n)$ are the probabilities of a radiative transition from the states A_ℓ and B_n, respectively. The second factor depends on the initial conditions and on the matrix elements of the interaction term $H(\underline{K}_o, \underline{e})$ which contains the multipole moments of the system.

If we return now to the probability amplitude $c_{p\rho\sigma}$, the square of its absolute value gives the probability of finding the nucleus in the final state C_p after it has emitted quanta into the ρ-th and σ-th field oscillators. If we sum over all the m-states of the final state, i.e. form $\sum_p < | c_{p\rho\sigma} | >^2_{av}$ then one finds the probability of the system emitting quanta into the ρ-th and σ-th field oscillators at any time t. One then takes the limit of the above sum as $t \to \infty$, i.e.

$$W_{\rho\sigma} = \lim_{t\to\infty} \sum_p < | c_{p\rho\sigma} | >^2_{av} , \qquad (1.9)$$

$W_{\rho\sigma}$ is then the probability of emission of quanta into the field oscillators ρ and σ. This quantity is important because from this we can find the probability that the second quanta will be emitted at an angle θ relative to the first.

This is done by integrating (1.9) over all the frequencies ν_ρ and ν_σ of the field oscillators. The first factor in $c_{p\rho\sigma}$ contains ν_ρ and ν_σ while the second contains the sole dependence on the directions of emission $\underline{K}_o'$ and $\underline{K}_o''$ and the polarizations $\underline{e}'$ and $\underline{e}''$. Hence after the integration over the frequencies one need only specify the second factor in $c_{p\rho\sigma}$ since one is interested only in relative probabilities.

It was mentioned in the introduction that directional-correlation measuring apparatus is polarization insensitive, thus one must sum over the polarizations $\underline{e}'$ and $\underline{e}''$. Further, it can be shown [(3) Appendix I p.130] that the value of the probability that two quanta will be emitted with a relative angle θ between them is independent of the direction that one chooses for the axis of quantization. Thus one can select the direction of propagation $\underline{K}_o'$ of the first photon as the axis of quantization $\underline{K}$ which yields

$$W = \sum_{\substack{\ell \\ e'}} \sum_{\substack{n \\ e''}} \sum_{p} | (j_1 | H(\underline{K},\underline{e}') | j) |^2 | (j | H(\underline{K}_o'',\underline{e}'') | j_2) |^2. \qquad (1.10)$$

This is the directional-correlation function which gives the probability that the second photon will be emitted at a relative angle θ to the first. One can notice that it contains the product of the squares of the absolute values of two matrix elements. These matrix elements contain the interaction term and of course, the multipole moments of the system. Thus the

multipole moment that determines the value of the matrix element $(j_1 \mid H(\underline{K},\underline{e}') \mid j)$ does not necessarily have to be that which determines $(j \mid H(\underline{K}_o'',\underline{e}'') \mid j_2)$, leading to the result that the photons can have multipolarities of different character.

The wave functions that enter into the calculation of the matrix elements in equation (1.10) depend on the quantum numbers $(j_1 m_1)(jm)$ and $(j_2 m_2)$. Let the first and second quanta carry away angular momentum in the amounts L_1 and L_2. Then $j_1 = j - L_1$ and $j_2 = j + L_2$. L_1 and L_2 are called the multipolarities of the radiations. Since (1.10) is summed over m_1, m, m_2 and the polarizations, then W depends on six quantities; the spins j_1 j and j_2 of the initial, intermediate and final states; the multipolarities L_1 and L_2 of the radiations and the angle θ that $\underline{K}_o$ makes with $\underline{K}$. Since θ is the independent variable, complete specification depends on j_1, j, j_2, L_1 and L_2.

Hamilton expresses the correlation function W in terms of powers of $\cos^2 \theta$, i.e.,

$$W = 1 + \frac{R}{Q} \cos^2 \theta + \frac{S}{Q} \cos^4 \theta \qquad (1.11)$$

where $\frac{R}{Q}$ and $\frac{S}{Q}$ are functions of $(j_1\ j\ j_2\ L_1\ L_2)$. He also evaluated $\frac{R}{Q}$ and $\frac{S}{Q}$ in terms of the spin j_1 of the initial state for various types of transitions. If we let $a_2 = \frac{R}{Q}$ and $a_4 = \frac{S}{Q}$ then

$$W = 1 + a_2 \cos^2 \theta + a_4 \cos^4 \theta. \qquad (1.12)$$

This expression holds when the cascade $j_1 \rightarrow j \rightarrow j_2$ is pure, i.e. each quantum is pure L_1 and L_2. When it is pure the cascade will be denoted by $j_1(L_1)\ j(L_2)j_2$.

According to Biedenharn and Rose (4) the most convenient form of describing the directional correlation $W(\theta)$ between gamma-rays g_1 and g_2 is:

$$W(\theta) = 1 + A_2 P_2 (\cos \theta) + \ldots + A_{k_{max}} P_{k_{max}} (\cos \theta). \qquad (1.13)$$

The highest term in this expansion is determined by the selection rules:

$$k_{max} = \text{Min } (2j,\ 2L_1,\ 2L_2).$$

The explicit calculation of the coefficients A_k is greatly facilitated by the fact that they can be broken up into two factors, each factor depending on only one transition of the cascade. Biedenharn and Rose denote these factors by F_k and write:

$$A_k = F_k(L_1\ j_1\ j)\ F_k(L_2\ j_2\ j)\ . \qquad (1.14)$$

Numerical values of the coefficients F_k have been calculated (4). Experimentally one determines the coefficients A_k by assuming an appropriate value for k_{max} (usually 4) and then making a least square fit of equation (1.13) to the values of $W_{exp}(\theta)$ measured at several angles.

The least squares fit is a technique that is well known and treated in many standard texts, (Snedecor, Statistical Methods, Iowa State College Press) hence, the results of the methods of least squares will be stated without proof or derivation. The matrix notation used in these statements is that of S. P. Lloyd's (S. P. Lloyd, private communication).

Consider the 3 x 5 matrix $\underline{A}$, where

$$\underline{A} = \begin{pmatrix} 1 & \cos^2\theta_1 & \cos^4\theta_1 \\ 1 & \cos^2\theta_2 & \cos^4\theta_2 \\ 1 & \cos^2\theta_3 & \cos^4\theta_3 \\ 1 & \cos^2\theta_4 & \cos^4\theta_4 \\ 1 & \cos^2\theta_5 & \cos^4\theta_5 \end{pmatrix}$$

The measurements are performed at angles $\theta_i (i=1,2,3,4,5)$. Let the transpose of $\underline{A}$ be $\underline{\tilde{A}}$. Then let $\underline{S} = \underline{\tilde{A}}\,\underline{A}$. $\underline{S}$ is then a 3 x 3 matrix. Next form the vector $\underline{\omega}$ where

$$\underline{\omega} = \begin{pmatrix} \omega_1 \\ \omega_2 \\ \omega_3 \end{pmatrix} = \begin{pmatrix} \sum_{i=1}^{5} W_M(\theta_i) \\ \sum_{i=1}^{5} W_M(\theta_i)\cos^2\theta_i \\ \sum_{i=1}^{5} W_M(\theta_i)\cos^4\theta_i \end{pmatrix} \qquad (1.15)$$

$$\omega_1 = \sum_{i=1}^{5} W_M(\theta_i) \qquad \omega_2 = \sum_{i=1}^{5} W_M(\theta_i)\cos^2\theta_i$$

$$\omega_3 = \sum_{i=1}^{5} W_M(\theta_i)\cos^4\theta_i$$

The function $W_M(\theta_i)$ is the measured correlation function. The product $\underline{S}^{-1}\ \underline{\omega}$ yields the vector that contains the uncorrected coefficients, i.e.,

$$\begin{pmatrix} a_o' \\ a_2' \\ a_4' \end{pmatrix} = \underline{S}^{-1} \begin{pmatrix} \omega_1 \\ \omega_2 \\ \omega_3 \end{pmatrix} \tag{1.16}$$

$\underline{S}^{-1}$ is the inverse of $\underline{S}$ and has the following form:

$$\underline{S}^{-1} = \begin{pmatrix} 0.8921 & -3.1997 & 2.3964 \\ -3.1997 & 23.0058 & -21.2884 \\ 2.3964 & -21.2884 & 20.9885 \end{pmatrix} \tag{1.17}$$

Thus the a_{2k}' are given explicitly by:

$$a_o' = 0.8921\omega_1 - 3.1997\omega_2 + 2.3964\omega_3 \tag{1.18}$$

$$a_2' = -3.1997\omega_1 + 23.0058\omega_2 - 21.2884\omega_3 \tag{1.19}$$

$$a_4' = 2.3964\omega_1 - 21.2884\omega_2 + 20.9885\omega_3 \ . \tag{1.20}$$

These equations yield the uncorrected coefficients a_{2k}' in terms of the measured correlation function and the independent variables $\theta_i (i=1,2,3,4,5)$.

The errors in these coefficients are found as follows. (S. P. Lloyd, private communication.) The deviation from the fitted curve is:

$$d_i = W_M(\theta_i) - (a_o' + a_2' \cos^2\theta_i + \ldots + a_{2k}\cos^{2k}\theta_i). \quad (1.21)$$

The cases of interest have k = 2 therefore:

$$\sum_{i=1}^{5} d_i^2 = \sum_{i=1}^{5} W_M^2(\theta_i) - (a_o' \sum_{i=1}^{5} W_M(\theta_i) + a_2' \sum_{i=1}^{5} W_M(\theta_i)\cos^2\theta_i +$$

$$+ a_4' \sum_{i=1}^{5} W_M(\theta_i)\cos^4\theta_i). \quad (1.22)$$

Multiply the matrix $\underline{S}^{-1}$ by $1/2 \sum_{i=1}^{5} d_i^2$. Then

$$\underline{E} = \frac{1}{2} \sum_{i=1}^{5} d_i^2 \, \underline{S}^{-1} . \quad (1.23)$$

$\underline{E}$ is called the covariant matrix of the estimates. The diagonal components of $\underline{E}$ are the squared deviations in a_o', a_2' and a_4'. Hence the standard deviations of a_o', a_2' and a_4' are the square roots of the corresponding diagonal components of $\underline{E}$. If $\sigma(a_o')$ is the standard deviation of a_o' then;

$$\sigma(a_o') = \sqrt{E_{11}} = \left\{ \frac{0.8921}{2} \sum_{i=1}^{5} d_i^2 \right\}^{1/2} \quad (1.24)$$

$$\sigma(a_2') = \sqrt{E_{22}} = \left\{\frac{23.0058}{2} \sum_{i=1}^{5} d_i^2\right\}^{1/2} \tag{1.25}$$

$$\sigma(a_4') = \sqrt{E_{33}} = \left\{\frac{20.9885}{2} \sum_{i=1}^{5} d_i^2\right\}^{1/2} \tag{1.26}$$

where $\sum_{i=1}^{5} d_i^2$ is given by (1.22). One could calculate the A_{2k} and their errors $\sigma(A_{2k})$ from equations (1.22) that express the A_{2k} in terms of the a_{2k} (note that Q, R and S correspond to a_o', a_2' and a_4' respectively) or one could go through a similar procedure as the one enumerated above for calculating the a_{2k} and their errors. All the errors in the a_{2k} and A_{2k} for all the correlations studied in Ni^{60}, W^{182}, Sm^{152} and Ta^{181} were calculated in the above manner. It should be noted that these errors include the measured correlation function and hence contain the experimental error in determining that function.

One can restrict the observation to the two angles $\theta = \frac{\pi}{2}$ and $\theta = \pi$. This measurement determines the anistropy

$$A = \frac{W(\pi) - W(\frac{\pi}{2})}{W(\frac{\pi}{2})} . \tag{1.27}$$

Assuming A_4 to be the highest coefficient in the expansion (1.13) the anisotropy A is related to the coefficients A_2 and A_4 by

$$A = \frac{1 + A_2 + A_4}{1 - \frac{1}{2} A_2 + \frac{3}{8} A_4} - 1. \tag{1.28}$$

The error in the anistropy contains the experimental error only. The errors in the coincidence method have been examined by A. C. G. Mitchell in Beta and Gamma-Ray Spectroscopy, Chapter VII, Interscience Publishers. His analysis is based on the fact that the error in the number of coincidences N_{12}^{T} is

$$e(N_{12}^{T}) = \frac{1}{T^{1/2}} [\Sigma N]^{1/2} \qquad (1.29)$$

where $N = N_T + N_{12}^{A} + N_{cosmic}$

N_{12}^{T} is the true number of coincidences

N_T is the total coincidence rate

N_{12}^{A} is the accidental coincidence rate

N_{cosmic} are the coincidences due to cosmic rays.

With this formula the errors in $W(\pi)$ and $W(\frac{\pi}{2})$ were obtained and the error in the anistropy calculated.

When formulas (1.24, 1.25, 1.26) are compared with (1.29) it is seen that if one takes the error in the anistropy as the error in the experiment it would be more accurate than the errors in the coefficients a_{2k} or A_{2k} since they contain the errors in the least squares fit.

It has been assumed that the nuclear cascade consists of two successive gamma-rays g_1 and g_2 (double cascade). More

than two gamma-rays are in cascade in many decays, and one can observe the correlation functions $W(g_1,g_2)$, $W(g_1,g_3)$ and $W(g_2,g_3)$. Biedenharn, Arfken and Rose (5,6) have extended the theory to this case. $W(g_1,g_3)$ can be written in the form (1.13) and values for the coefficients A_k are given in Table XI of reference (4). There are cases where the observation of $W(g_1,g_3)$ can be used to decide on the order of emission of the gamma-rays. There are also cases where the correlation function is independent of the order of transition. (7,8)

We shall consider now the directional correlation for double cascades in which one of the two gamma-rays is mixed. Suppose the first transition in a cascade to consist of a mixture of L and $L' > L$ with a mixing ratio δ. This δ is defined as the ratio of the matrix elements.

$$\delta = (j \,||\, L' \,||\, j_1)/(j \,||\, L \,||\, j_1). \qquad (1.30)$$

The ratio of the total intensity of the L' pole to that of the L pole is then equal to δ^2. Since the matrix elements are chosen to be real the mixing ratio δ is real, however, for a given intensity ratio δ^2, the mixing ratio δ can have either a positive or negative sign, depending on the relative phase of the matrix element. An important item here is that the sign depends on how the matrix elements are defined. The matrix elements $(j \,||\, L' \,||\, j_1)$ are reduced matrix elements in that the matrix element $< jm \,|\, L' \,|\, j_1 m_1 >$ has been reduced to $(j \,||\, L' \,||\, j_1)$

by the Wigner-Eckart theorem. The L′ indicates an operator of degree L′. [(4) footnote (6)].

The directional correlation function for the cascade $j_1(L_1\ L_1')\ j(L_2)j_2$ can be written as

$$W(\theta) = W_I + \delta^2\ W_{II} + 2\delta W_{III} \tag{1.31}$$

where W_I and W_{II} are correlation functions for the pure cascades $j_1(L_1)\ j(L_2)j_2$ and $j_1(L_1')\ j(L_2)j_2$. These can be evaluated from equations (1.13) and (1.14). W_{III} is due to the interference between L_1 and L_1' and is given by

$$W_{III} = \sum_{\substack{k\neq 0 \\ \text{even}}} A_k^{III}\ P_k(\cos\ \theta) \tag{1.32}$$

with

$$F_k(L_1L_1'j_1j) = (-1)^{j-j_1-1}\left[(2j+1)(2L_1+1)(2L_1'+1)\right]^{1/2}\ G_k(L_1L_1'j_1j). \tag{1.33}$$

The function $G_k(L\ L'\ j_1j)$ has been calculated for the case $L' = L + 1$ by Biedenharn and Rose (4). Thus $W(\theta)$ can again be written as in equation (1.13).

This discussion of the theory of gamma-gamma directional correlation will be terminated by recording without derivation the transformations which enable one to express the

coefficients A_k of the group-theoretic formalism in terms of the coefficients a_k of the Hamilton formalism and vice versa. Thus the correlation function can be expressed in either of the forms:

$$W(\theta) = Q + R \cos^2\theta + S \cos^2\theta$$

$$W(\theta) = A_o' + A_2' P_2(\cos\theta) + A_4' P_4(\cos\theta) \qquad (1.34)$$

where the transformation equations are:

$$A_o' = Q + \frac{1}{3} R + \frac{1}{5} S; \quad A_2' = \frac{2}{3} R + \frac{4}{7} S; \quad A_4' = \frac{8}{35} S \qquad (1.35)$$

$$A = A_o' - \frac{1}{2} A_2' + \frac{3}{8} A_4'; \quad R = \frac{3}{2} A_2' - \frac{30}{8} A_4'; \quad S = \frac{35}{8} A_4' \qquad (1.36)$$

$$a_2 = \frac{R}{Q} \qquad a_4 = \frac{S}{Q} \qquad A_2 = \frac{A_2'}{A_o'} \qquad A_4 = \frac{A_4'}{A_o'} \quad .$$

The a_k are used for graphical analysis and the A_k for determining spin assignments and mixing ratios.

(c) Collective Model of the Nucleus

The collective model of the nucleus is a model that attempts to explain the occurrence of rotational spectra in nuclei with high Z. The theory as presented by G. Alaga et al (47) can predict the energies and spin sequences of the various nuclear states along with the relative strengths of the transitions from a given nuclear state to those states which belong to a rotational band. The strengths of the transitions which take place within a given rotational band can also be calculated.

The intensity rules developed by this theory for beta and gamma transitions to nuclear rotational states are rather simple and have developed into a powerful aid for classifying decay schemes.

This thesis is concerned with the collective model of the nucleus because the three isotopes that are studied have atomic numbers that lie in the region $60 \leq Z \leq 92$ which is called the "strong coupling region." This region does not follow the predictions of the shell model of the nucleus but it does seem to follow those predictions made by the collective model. Thus the spins of the nuclear states and the multipolarities of the gamma-radiations that are measured by directional correlation methods can be used to test the collective model if the measurements are made on nuclei that lie in the strong coupling region.

The basic approach to the problem of calculating the intensity rules is based on the spherical symmetry of the

nucleus. Nuclei with a $60 \leq Z \leq 92$ appear to have a large number of nucleons that are not in closed shells, enough evidently to give the nucleus a large equilibrium deformation. It is then deduced that the rotational spectra depends on this equilibrium deformation. Nuclei that are so deformed can be excited into two different modes; the intrinsic and the rotational.

The rotational spectrum depends on the collective or combined motions of all the nucleons. This motion only affects the orientation of the nucleus relative to some space fixed axis. The motion for axially symmetric nuclei because of this reason can be represented by three quantum numbers, j, K and M, where j is the total angular momentum, K is its projection on the nuclear symmetry axis and M is its projection on the space fixed axis.

The intrinsic mode of excitation refers to the excitation of the individual nucleons or with so-called collective vibrations of the nuclear shape. Alaga et al (47) have shown that the same intrinsic wave function represents the states in a rotational band which have different j-values. This is a consequence of assuming that the intrinsic and rotational excitations can be separated by representing the solution of the nuclear wave equation by the product of an intrinsic wave function and a rotational wave function.

When the nuclear wave equation is not separable into intrinsic and rotational parts the rotational spectra is no

longer independent of the intrinsic structure. The dependency of the rotational spectra on the intrinsic structure is examined by using perturbation methods, i.e. the perturbed wave function is assumed to consist of the sum of an unperturbed wave function and a term which represents a mixing of the intrinsic and rotational states. The unperturbed wave function is just the solution of the separable nuclear wave equation. The analysis reveals that the perturbing term which consists of the mixing of states seriously affects the intensity rules if the transition probabilities for the unperturbed case are small or zero.

If they are zero then the perturbing term alone determines the transition probabilities for a transition from a given nuclear state to those states that belong to a rotational band or for transitions within a given rotational band. These transition probabilities contain matrix elements of both the intrinsic and rotational structure. Evidently the contribution of the intrinsic matrix elements is such that they reduce the transition probabilities or retard the transition. This is done by putting certain restrictions on K (the projection of the total angular momentum j on the nuclear symmetry axis) hence these transitions are called K-forbidden. The concept of K-forbiddenness is important here because many of the gamma radiations in W^{182} are K-forbidden.

Returning to the case of rotational spectra independent of the intrinsic structure (separable nuclear wave

equation), odd-A nuclei have K values that are positive half integer which permits j to take on values:

$$j = K,\ K + 1,\ K + 2,\ \ldots. \tag{1.37}$$

and all of these states have the same parity as the intrinsic structure.

Even-even nuclei have K = 0 in the ground state and symmetrization of the wave function limits the rotational band to

$$j = 0,2,4,6,\ldots. \text{ even parity.} \tag{1.38}$$

The quantum number K is not zero in an odd-odd nucleus or in excited intrinsic states of even-even nuclei. Hence the rotational sequence is again given by (1.37).

Classification of gamma transitions adheres to convention in that they are classified in terms of electric and magnetic multipole orders (E_L and M_L). The parity is:

$$\pi = (-)^L \quad \text{for } E_L$$

$$\pi = (-)^{L+1} \quad \text{for } M_L \ .$$

The selection rules that apply to L and π for a gamma transition from a state with quantum numbers (K_i, j_i, π_i) to a state with (K_f, j_f, π_f) are:

$$| j_i - j_f | = \Delta j \leq L \leq j_i + j_f \qquad \pi = \pi_i \pi_f \tag{1.39}$$

$$| K_i - K_f | = \Delta K \leq L. \tag{1.40}$$

The selection rules for j and π are binding for this case (separable nuclear wave equation) and for the case where the nuclear wave equation is not separable.

The selection rule for K however depends on the adequacy of the wave function. This means that small variations from the separable rotational wave function removes the stringency of the selection rule for K which then only acts to retard rather than completely forbid the corresponding multipole transition, i.e. the transitions are K-forbidden. The degree of forbiddenness is characterized by the number ν where

$$\nu = \Delta K - L \ . \tag{1.41}$$

(d) The Treatment of Experimental Data

The measured correlation function $W_{exp}(\theta)$ corresponds to the theoretical correlation function $W(\theta)$ only when one assumes centered point sources, point detectors, no scattering and no interfering radiations. One must correct the experimental data for the various deviations from such an ideal arrangement in order to compare experimental and theoretical results.

The first obvious effect to be corrected for in angular correlation work is scattering. Scattering effects can mask the true correlation. Suppose the radiation is scattered in the source. Two effects mask the correlation function;

(i) Some of the gamma-rays are deflected before being counted. This is caused by Compton scattering and tends to "smear out" the correlation, thus it always decreases the magnitude of the coefficients A_k.

(ii) The pairs of gamma-rays which give coincidences in the 180° position are absorbed more readily in the source than those that yield coincidences in the 90° position. Hence more coincidences are missed at 180° than at 90°. Further, a correlation function with negative anistropy is attenuated. The photoelectric effect is the main cause of absorption. The Compton effect also accounts for some absorption because the gamma-rays lose so much energy that they are no longer counted. This absorption is accentuated for low gamma-ray energies and sources with high atomic number Z. One can eliminate effect (ii) by using a thin

radioactive source, however, if it is surrounded by scattering material effect (i) is present and the correlation is attenuated.

Experimentally one finds the unperturbed correlation function by measuring the anistropy for different source diameters and making a plot of it against the probability that a gamma-ray pair will escape from the source without undergoing either photoeffect or Compton effect. In most correlation experiments, however, the source can be chosen so that no correction for source size is necessary. One may be forced to use large sources because of very small specific activities, then the consideration of effects (i) and (ii) applies. The sources used by the author in his experiments were such that correction for source size was not necessary.

Besides scattering in the source, scattering of any radiation in or near the counters can give rise to spurious coincidences (9). These are not isotropic and hence simulate a correlation. One can avoid such accidental coincidences by shielding the counters with cone-shaped lead shields which accept only the gamma-rays from a point source. A slight error in positioning the source however changes the solid angle to a large extent. Hence the lead shields should be built in a manner that source size and slight decentering do not affect the solid angle. The best protection against scattered gamma-rays and spurious coincidences consists in using differential discriminators to accept only the photopeaks of the desired gamma-rays.

Both differential discriminators and lead shields were used in these investigations.

Before a given experiment was performed, the resolving time τ_R and the background were determined. N_1 and N_2 denote single counts in channels 1 and 2 and N_{12} denotes the coincidences between them. For accurate measurements the ratio of true coincidences N_{12}^T to accidental N_{12}^A should be larger than 5 to 1; under unfavorable conditions one may be forced to make it as high as unity. One obtains the true value N_{12}^T by subtracting background and accidental coincidences and if necessary any contributions due to disturbing radiations. The coincidence ratio $N_{12}^T/N_1\ N_2$ is then formed (10). This ratio is independent of the decay of the source and corrects small errors in centering the source. The coincidence ratio $N_{12}(\theta)$ is then fitted by an expansion of the form (1.13). Rose (11) has thoroughly treated the determination of the coefficients A_k' by a least square fit, and also the calculation of the errors in A_k and the determination of k_{max}. The last step consists in correcting the coefficients A_k' for the finite solid angle of the counters.

Lawson and Frauenfelder (12) found that the measured directional correlation function depended strongly on the settings of the pulse-height discriminators in the counting system. In order to explain this result, they assumed that the effective solid angle depends on the pulse-height selection and measured the angular resolution curves of the radiation detectors. Once the effective angular resolution curves were found, they calculated

the correction for their source. Their calculation showed that the discrepancy actually was due to different solid angles. This result proved that a solid angle correction without experimental determination of the angular resolution of the counters for the radiation to be investigated may cause serious errors. The solid angle correction has been treated in various approximations by Walter (13,14), Frankel (15,16), Church and Kraushaar (17), and Rose (18). These papers provide sufficient theoretical background for the treatment of almost all experimental arrangements. The results of Lawson and Frauenfelder (12) are presented here.

It is assumed that one is measuring the directional correlation $W(\theta)$ of successive gamma-rays g_1 and g_2. The experimental arrangement consists of a point source in the center of the counting system (Fig. 1) and of two circular (cylindrically symmetric) scintillation counters. The axes of the two counters subtend the angle φ at the source, the directions of emission of the two gamma-rays include the angle θ. The efficiency of a counter for a gamma-ray emitted at an angle α with respect to the counter axis shall be denoted by $\varepsilon(\alpha)$. The efficiency $\varepsilon(\alpha)$ is also a function of the source-to-counter distance. This distance must be kept the same for the measurement of both the directional correlation and of the angular resolution. The theoretical directional correlation function $W(\theta)$ may be written as:

$$W(\theta) = 1 + \sum_{k=1}^{m} A_{2k} P_{2k}(\cos \theta) \qquad (1.42)$$

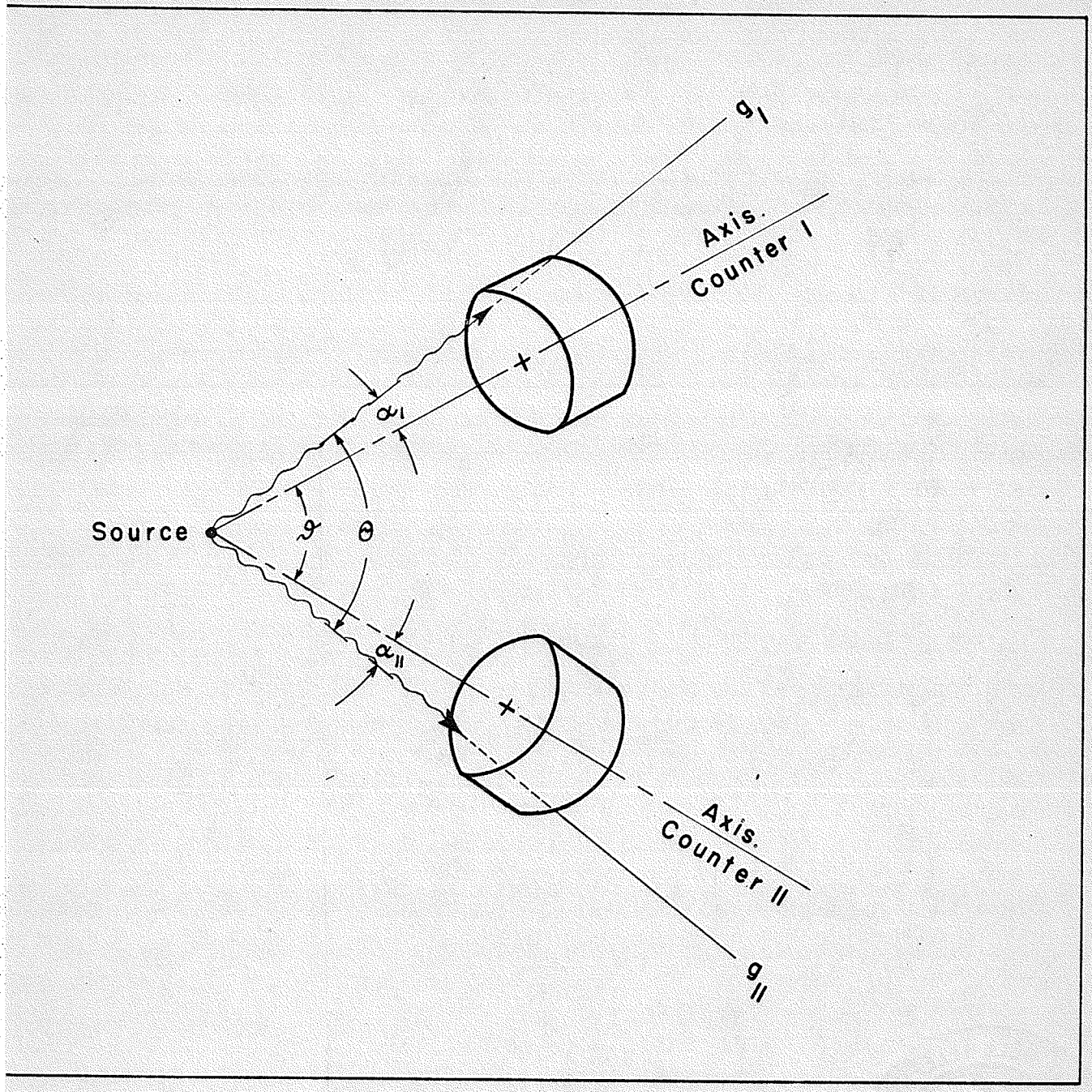

Fig. 1. Geometry of the detecting system for the measurement of the directional correlation between g_1 and g_2. Taken from Lawson and Frauenfelder (12).

It was first shown by Frankel (15) that the experimentally measured or "smeared out" directional correlation $< W(\varphi) >_{av}$, where φ is the angle between the counter axes, can be written as

$$< W(\varphi) >_{av} = Q_o + \sum_{k=1}^{k_m} Q_{2k} A_{2k} P_{2k}(\cos \varphi). \qquad (1.43)$$

The coefficients A_{2k} of the theoretical function are multiplied by appropriate attenuation factors Q_{2k}. This procedure is valid only for centered point sources and circular detectors. Walter (13,14) has shown that a mixing of the different A_{2k} occurs if these conditions are not met.

For gamma-rays of approximately the same energies, i.e. $\varepsilon(\alpha,g_1) \cong \varepsilon(\alpha,g_2)$ the attenuation factors can be written as

$$Q_{2k} = J^{1}_{2k} J^{11}_{2k} \qquad (1.44)$$

with

$$J_{2k} = \int P_{2k}(\cos \alpha)\varepsilon(\alpha) \mid \sin \alpha \mid d\alpha \qquad (1.45)$$

where the integrals J^{1}_{2k} and J^{11}_{2k} are evaluated respectively for the first and second counters. When the gamma-ray energies are different expression (1.44) must be replaced by

$$Q_{2k} = \frac{1}{2} \left\{ J^{1}_{2k}(g_1)\, J^{11}_{2k}(g_2) + J^{11}_{2k}(g_1)\, J^{1}_{2k}(g_2) \right\}. \qquad (1.46)$$

The procedure for correcting a measured correlation is now obvious. The angular efficiencies $\varepsilon^{I}(\alpha)$ and $\varepsilon^{II}(\alpha)$ of the counters have to be measured by means of a collimated beam of gamma-rays of the substance to be investigated. If g_1 and g_2 differ considerably in energy, two different gamma-sources with suitable energies have to be used to determine $\varepsilon(\alpha,g_1)$ and $\varepsilon(\alpha,g_2)$. The correction factors Q_{2k} are found by integrating equation (1.45) numerically using the experimentally determined angular efficiencies. The coefficients A_2' and A_4' are obtained from a least squares fit of the experimentally measured correlation $< W(\varphi) >_{av}$. The corrected coefficients are then given by

$$A_{2k} = \left\{\frac{Q_o}{Q_{2k}}\right\} A_{2k}' \quad . \tag{1.47}$$

If the energies of the gamma-rays g_1 and g_2 are close to the energy of annihilation radiation the method of Church and Kraushaar (17) may be used. The angular resolution $F(\alpha)$ of the counter system for a source emitting annihilation radiation has to be measured. Q_{2k} is then given by equation (1.45) with $\varepsilon(\alpha)$ replaced by $F(\alpha)$. These methods hold only for centered sources.

The angular resolution corrections are the most important corrections to be applied to the experimental data and were used throughout the thesis.

Chapter II

Coincidence Method

(a) Coincidence Spectrometry

A coincidence circuit is used in the following manner. Output pulses from two nuclear counters are used to drive a coincidence unit which is required to give an output pulse every-time a pulse from one counter arrives within a given short time interval of a pulse from the other counter. This time interval is called the "coincidence resolving time." The resolving time usable for a given arrangement depends upon the kind of phosphor and the energy of the radiation. For stilbene $\tau = 10^{-9}$ seconds is usable down to 25 kev, for NaI(TL) $\tau = 3 \times 10^{-9}$ seconds down to an energy of 50-100 kev and $\tau = 10^{-8}$ seconds down to 10 kev. These times are considerably shorter than is usually considered usable with NaI(TL) and are made possible by circuit arrangements which depend for their timing upon the arrival of the first few photoelectrons after amplification in the photomultiplier. Morton (19) has shown that much more precise timing is possible using the first few electrons rather than using the mean time of the photomultiplier pulse as do the coincidence arrangements using no integration followed by pulse limiting. The measurement of the angular correlation of certain gamma-ray cascades is an experiment which illustrates the use of a coincidence circuit and the importance of a short stable resolving time.

Let N be the average number of nuclear disintegrations occurring per second and let the two types of gamma-ray be denoted by g_1 and g_2. The number of output pulses from counter I due to g_1 quanta is then $N\varepsilon_1\omega_1$, where ε_1 is the efficiency of the counter and ω_1 is the solid angle subtended by the counter at the source. A fraction of these nuclei will give a g_2 quantum traveling towards counter II so that a coincidence output counting rate of

$$N_c = N\ \varepsilon_1\ \varepsilon_2\ \omega_1\ \omega_2\ W(\theta) \tag{2.1}$$

will be obtained. Let $e_1 = \varepsilon_1\omega_1$ and $e_2 = \varepsilon_2\omega_2$. ε_2 is the efficiency of counter II and ω_2 is the solid angle subtended by counter II at the source. Then,

$$N_c = N\ e_1e_2\ W(\theta) \tag{2.2}$$

$W(\theta)$ is the correlation function and is a function of the angle between the two counters. If there is no preferred angle between the two gamma-rays then $W(\theta)$ is unity. When a system does not have pulse height discrimination in both channels, counter II may register a g_1-ray and give a coincidence output with a g_2-ray passing through counter I, hence we have:

$$N_c = 2N\ e_1e_2\ W(\theta). \tag{2.3}$$

This is assuming that the counter efficiencies for the two types of gamma-ray are the same and no pulse height discrimination exists in either channel.

If there are pulse height discriminators in both channels and the discriminator in channel I is set to accept the photopeak due to g_1 while the discriminator in channel II accepts only the photopeak due to g_2 then obviously counter I can only count those pulses due to g_1 quanta and counter II those due to g_2. The coincidence output is then:

$$N_c = N\ \varepsilon_1\varepsilon_2\ \omega_1\omega_2\ x\ W(\theta) \tag{2.1}$$

or

$$N_c = N\ e_1 e_2\ W(\theta). \tag{2.2}$$

The factor 2 present in (2.3) thus drops out.

In addition to these genuine coincidences some output signals will be produced due to accidental coincidences between pulses from the two counters. Thus

$$N_{12}^A = 2N_1N_2\tau \tag{2.4}$$

where

N_{12}^A = accidental ~~coincidences~~ coincidence rate.

N_1 = singles counting rate for counter I

N_2 = singles counting rate for counter II.

The factor 2 in this relation arises because the coincidence unit operates if a pulse from B arrives within the time interval τ of a pulse from counter I, irrespective of which pulse occurs

first. Consider next the genuine to accidental coincidence ratio for no pulse height discrimination in either channel. Then

$$N_1 = 2\,Ne_1 \qquad (g_1 \text{ and } g_2 \text{ quanta})$$

$$N_2 = 2\,Ne_2 \qquad (g_1 \text{ and } g_2 \text{ quanta}) .$$

Therefore substituting these into equation (2.4)

$$N_{12}^A = 8N^2\, e_1\, e_2\, \tau$$

but

$$N_c = 2N\, e_1\, e_2\, W(\theta) \tag{2.3}$$

when no pulse height discriminations exist. Hence

$$\frac{N_c}{N_{12}^A} = \frac{W(\theta)}{4N\tau} . \tag{2.5}$$

We shall now consider this ratio when both channels do contain discriminators. Thus

$$N_1 = N\, e_1 \qquad (g_1 \text{ quanta only})$$

$$N_2 = N\, e_2 \qquad (g_2 \text{ quanta only}) .$$

Substituting these expressions into equation (2.4) yields

$$N_{12}^A = 2N^2\, e_1\, e_2\, \tau \tag{2.6}$$

and hence

$$\frac{N_c}{N_{12}^A} = \frac{W(\theta)}{2N\tau} \quad . \tag{2.7}$$

Hence we arrive at two distinct formulae for the two cases. The $W(\theta)$ is not the same in both cases, however. The angular correlation function in (2.7) is the fraction of the pulses in the portion of the spectrum accepted by one differential discriminator that is related by coincidence to the radiation being accepted by the other discriminator. In (2.5) the whole spectrum is in coincidence through the two channels. Thus it can be seen that it is necessary to keep N as high as possible so that the true coincidence rate is high enough to give a sufficient number of counts for adequate accuracy in a reasonable experimental time. This rate is proportional to the solid angle of collection by the counters, so that in order to achieve good angular resolution, N must be increased to a maximum in order that this solid angle may be kept small. Equation (2.7) shows that τ the coincidence resolving time must accordingly be reduced to a minimum. It should be noted that since N_{12}^A is a function of τ, τ must be kept constant during the experiment in order that a correction may be made to the experimental results to allow for accidental coincidences.

(b) The Apparatus

The spectrometer to be described is a three channel coincidence spectrometer. The principle of operation is fundamentally the same as that of the two channel system. The detailed functioning of the three channel system will be discussed later.

Plate I is a photograph of the complete unit. The unit on the small table on the right hand side is the Sorenson 50-60 cycle A.C. regulator. The contents of the floor rack are as follows: The top unit is a potentiometer type 1007 which is used to adjust the voltage on the photomultiplier tubes. The unit below the potentiometer is the high voltage power supply, a Hamner model N-401. The third unit from the top in the rack is a conventional Atomic glow transfer scaler while the bottom unit is the Harwell coincidence unit type 1036A. The table in the foreground contains an Atomic model 1005 scaler and a Fischer and Marshall (20) type coincidence unit. The table that supports the photomultiplier tubes contains two power supplies at the rear. The one at the right rear provides plate and filament voltage to the Roulston type (21) differential discriminator just in front of it. The power supply at the left rear provides plate and filament voltage to two amplifiers and one of the cathode followers mounted at the base of the photomultiplier tubes. The two smaller units to the left of the differential discriminator and in front of the left rear power supply are amplifiers

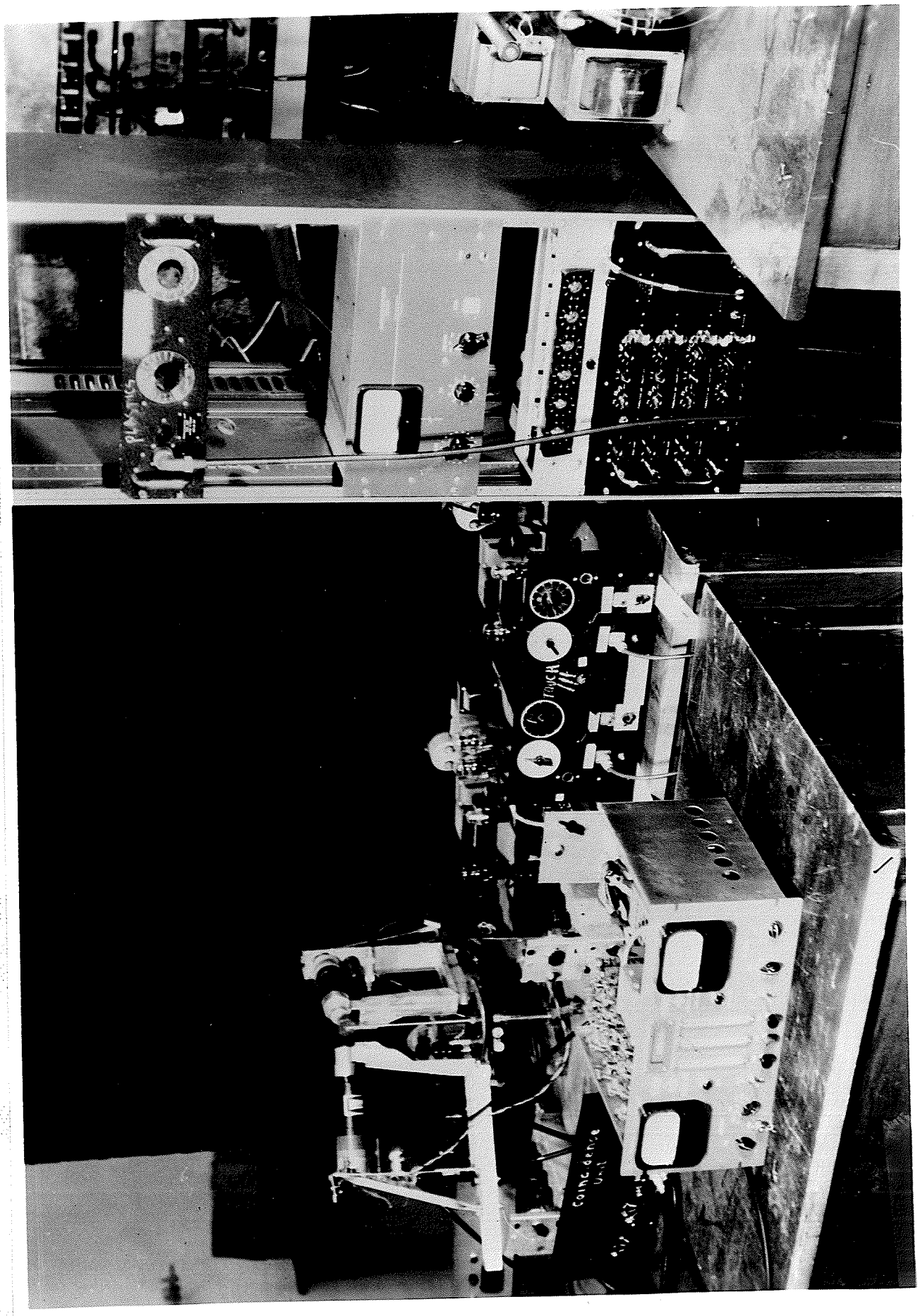

Plate I

The Fast-Slow Coincidence Spectrometer

similar to one loop of Atomic's amplifier model 204C. The photomultiplier tubes are to the left of these amplifiers; they are mounted on aluminum brackets which are secured to a spectrometer (optical) bench. The two small units on the left of the spectrometer bench on the adjoining table are amplifiers of the type previously mentioned. The power supply behind them and to the left provides their plate and filament supply while on the extreme left there is a Lambda type that provides power for the coincidence unit.

Plate II is a close-up of the spectrometer bench. The graduated circle on the bench permits the determination of the position of the movable counter (right hand side) to the nearest 30 minutes (1/2 degree). The photomultiplier on the left is fixed and is a DuMont K1185. The movable photomultiplier is a ~~Dumont~~ DuMont 6292. A brass rod supports the source which is mounted in a circular lead disk or back-scatter shield. The crystals used in the detectors are 1" x 1" right circular cylinders of thallium-activated sodium iodide mounted by and purchased from the Harshaw Chemical Co. The containers of these crystals are thin aluminum caps with magnesium oxide filler between the crystal and container walls to act as a diffuse reflector. Glass end windows completed the crystal mountings. The mounted crystals were secured to the photomultiplier windows with spring loaded aluminum spinnings (24). Heavy Dow Corning silicone grease was used as an optical bond between the crystals and the photomultiplier windows. The aluminum spinnings were taped into

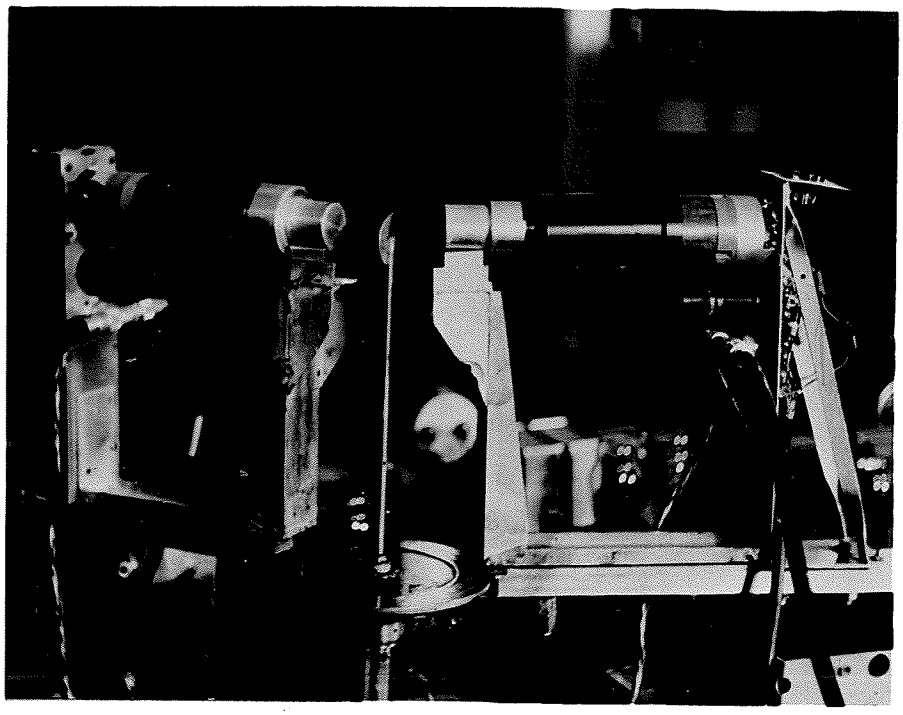

Plate II
The photomultipliers, the source, back-scatter shield and spectrometer bench.

position with black electrical tape which also acted as a light tight cover for the photomultiplier. The lead conical shields were 0.44 inches thick along their sides with a tapered face of 0.62 inches thickness which had a tapered hole bored through its center. The inner end of this hole has a diameter of 0.90 inches, the outer 0.70 inches in diameter.

The lead disk was 1/4 inch thick and 1-1/2 inches in diameter. A tapered hole 3/16 inches in diameter was bored through its center and the source was sealed into the hole with paraffin wax. The spectra under examination had the usual single and multiple Compton back-scattered components found with single crystal spectrometers, however the Compton scattering from detector to detector produced false coincidences. For instance a Compton process in crystal 2 could give rise to a back-scattered photon in crystal 1. The scattering situation is not improved by increasing the source to detector distance since the coincidence rate decreases as fast as the scattering. The back-scattering or anti-Compton shield considerably reduces the effect (22). This anti-Compton shield is a lead plate with a central hole in it to support the source. The scattered photon must then either pass through the source or the shield to reach the other detector.

For circuit details on the differential discriminator, pulse amplifiers, the Harwell type coincidence unit 1036A, the cathode follower and the photomultiplier circuitry see references (21), (23) and (24). The existing apparatus was improved

over that used by Taylor (24) by the introduction of a third channel, but more important by the use of a Sorenson A-C regulator and a Hamner High Voltage Power Supply Model N-401. The Sorenson A.C. regulator requires 95 to 130 volts A.C. input voltage and gives an output voltage of 115 volts plus or minus one-tenth of one percent. This unit provided regulated line voltages to all the units in the laboratory that required high stability such as the Hamner N-401, the power supply for the Roulston type differential discriminator, the Harwell coincidence unit 1036A etc. The Hamner N-401, which provided the high voltage for the photomultiplier tubes, requires 115 volts at 50-60 cycles. It received this from the Sorenson. The N-401 can give a positive or negative output between 500 to 1800 volts, continuously variable. It regulates to within 2.5 parts per million per milliampere through a range 0 to 5 milliamps (1000 volts output). Its stability against line voltage changes is 3 parts per million per volt in 105 to 125 volt range (1000 volts output). However, since it received its line voltage from the Sorenson stability was no longer a problem. The noise and ripple is less than 3 parts per million peak to peak. (1000 volts output).

This power supply is a marked improvement over the A.E.R.E. model 1007 supplying -2000 volts with a possible variation of ± 0.1% fluctuation in ~~line~~ output voltage that Taylor (24) used. Taylor also mentions (25) that the overall stability of his apparatus was poor, a given photoelectron line drifting as much as 5% during a 24-hour period. With the new equipment the drift was

reduced to one-tenth of one percent per 24-hour period. This high stability, high regulation apparatus accounts for the success the author of this thesis achieved with W^{182} and Sm^{152}.

The three-channel coincidence spectrometer is also called a "fast-slow" coincidence system since it combines the assets of a fast-coincidence system with that of a slow coincidence system. The assets of a fast-coincidence system is that it has a short resolving time, i.e. 10^{-8} to 10^{-10} seconds, and it relies on its operation by the pulse derived from the first few photoelectrons produced in the photomultiplier tube. The slow-coincidence system has the advantage of being able to select by pulse-height discrimination the gamma-rays that are to be studied. A disadvantage is that the discriminator requires an input pulse proportional to the total number of photoelectrons released by the light scintillation from the phosphor. Thus the discriminator output pulse will be delayed with respect to the pulse operating the fast coincidence unit and this delay will vary with pulse height. The fast coincidence circuit therefore cannot follow the pulse-height discriminator as in the case of slow coincidence circuits. The fast-slow system combines the merits of both by using the fast system to determine the resolving time and the slow to perform the necessary pulse-height discrimination. This requires three coincidence mixers, one fast and two slow. The fast coincidence mixer will now be described.

The coincidence circuit proper consists of a 6BN6 Tube alone (Fig. 2). The control grids G_1 and G_3 are terminated by

200-ohm resistors between each grid and ground. The cathode is connected to ground through a by-passed 2500-ohm potentiometer which may be adjusted to give the necessary cathode bias. It may also be used to control pulse-height selection. The cathode bias is unaffected by the fact that plate-current is normally cut-off, because the cathode current flows to the accelerating electrode, and its magnitude is almost completely determined by the voltage there. The accelerating electrode G_2 is connected to a source of positive voltage, and the plate is connected to the same source through a 330k resistor.

When used as a coincidence mixer the tube is operated below cut-off. If a positive pulse of sufficient size is applied to G_1 a burst of electrons passes through and arrives a short time later at G_3. If G_3 should receive a positive pulse at the instant the electrons arrive from G_1 electron current can reach the plate and change its potential by an amount proportional to the charge received and inversely to the capacitance of the plate circuit. The charge on the plate then leaks off with a time constant equal to the RC of the circuit. The pulse at the plate is fed to the associate electronic equipment through a cathode follower. The input pulses were clipped by shorted delay lines 1/2 foot in length, made of RG-176/U coaxial cable with a delay of 0.1 microseconds per foot and a characteristic impedance of 2,000Ω. The input pulse after delay line clipping has a width $\sim 2T_cL + T_r$ where T_r is the rise time of the original pulse and T_c is the delay time per foot. L is the length of the delay line

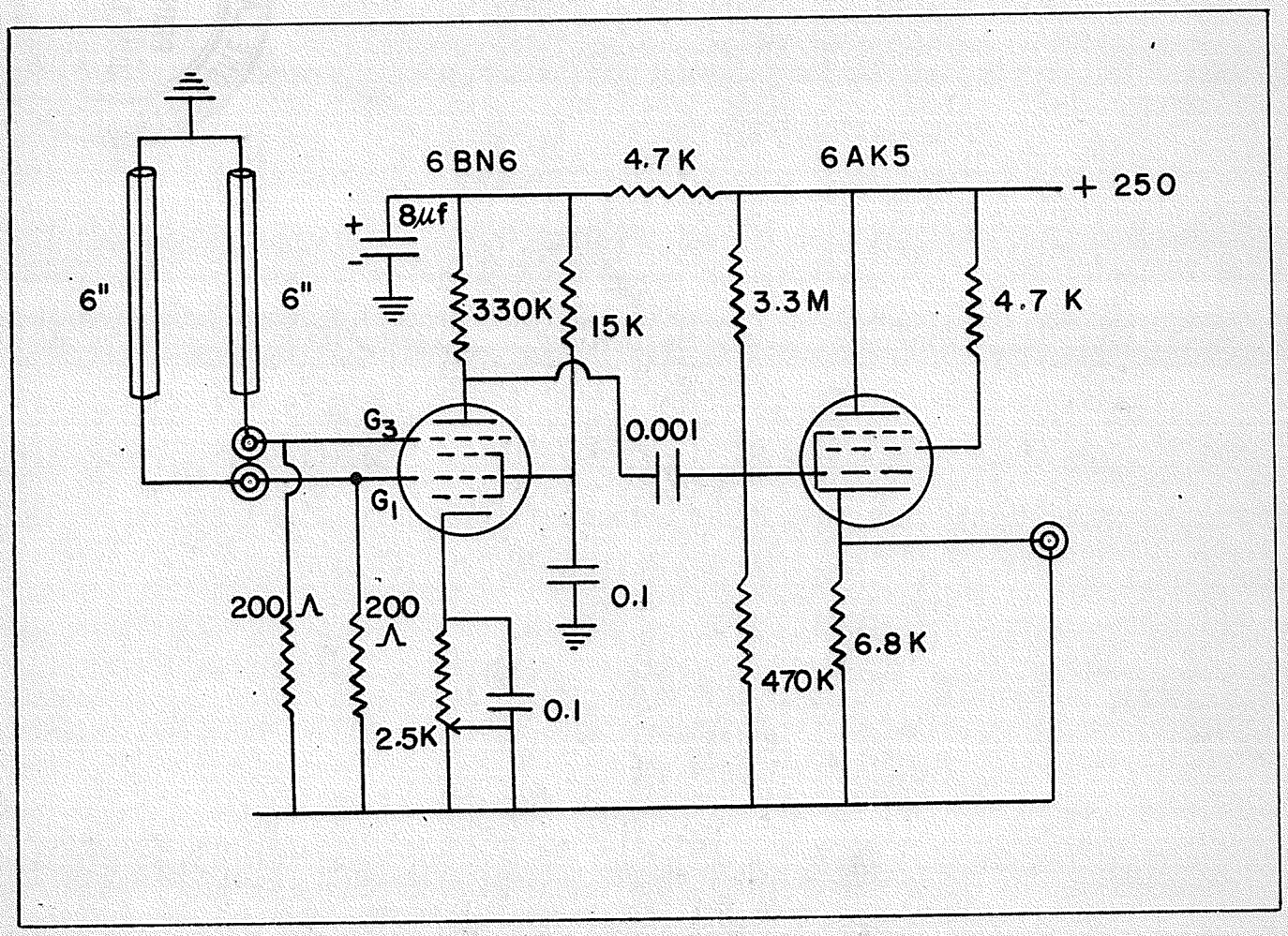

Fig. 2. Diagram of 6BN6 coincidence circuit. Except for the delay line clipping this is essentially the circuit designed by Fischer and Marshall (26).

in feet. When $T_r >> T_c$ then the pulse width is $\sim 2T_cL$. Thus with T_c = 0.1 microsec/ft. and L = 1/2 ft. the maximum width of the input pulses to the 6BN6 was 10^{-7} seconds. Pulse height selection was used in the form of cathode bias, thus only the upper portions of these pulses were used as triggering pulses, and they were of width $\sim 2x10^{-8}$ seconds. Thus a resolving time of $2x10^{-8}$ seconds was obtained. Fischer and Marshall (20) found that a slightly higher bias was required to reject single pulses applied to G_1 than to G_3. This was used to an advantage later on when the author was seeking coincidences between pulses of different pulse height.

The fast-slow coincidence circuit is illustrated diagrammatically in Fig. 3. Consider gamma-rays g_1 and g_2 that are in cascade. The spectrum of the source to be studied that contains this cascade is obtained with each channel of the slow unit. Then the differential discriminator in channel 1 is set to accept the photopeak due to g_1 and the discriminator in channel 2 is set to accept the photopeak due to g_2. The output pulses from the discriminators are then fed into channels 1 and 2 respectively of the three channel coincidence unit 1036A. The delays in these channels are adjusted so that the maximum number of coincidences is obtained in the first mixer which was operated with a resolving time 0.5 microseconds. These same pulses due to g_1 and g_2 are clipped by shorted delay lines, amplified, clipped again and then mixed by the fast Fischer and Marshall Type unit with a τ of $2x10^{-8}$ seconds. The output pulse from this unit is

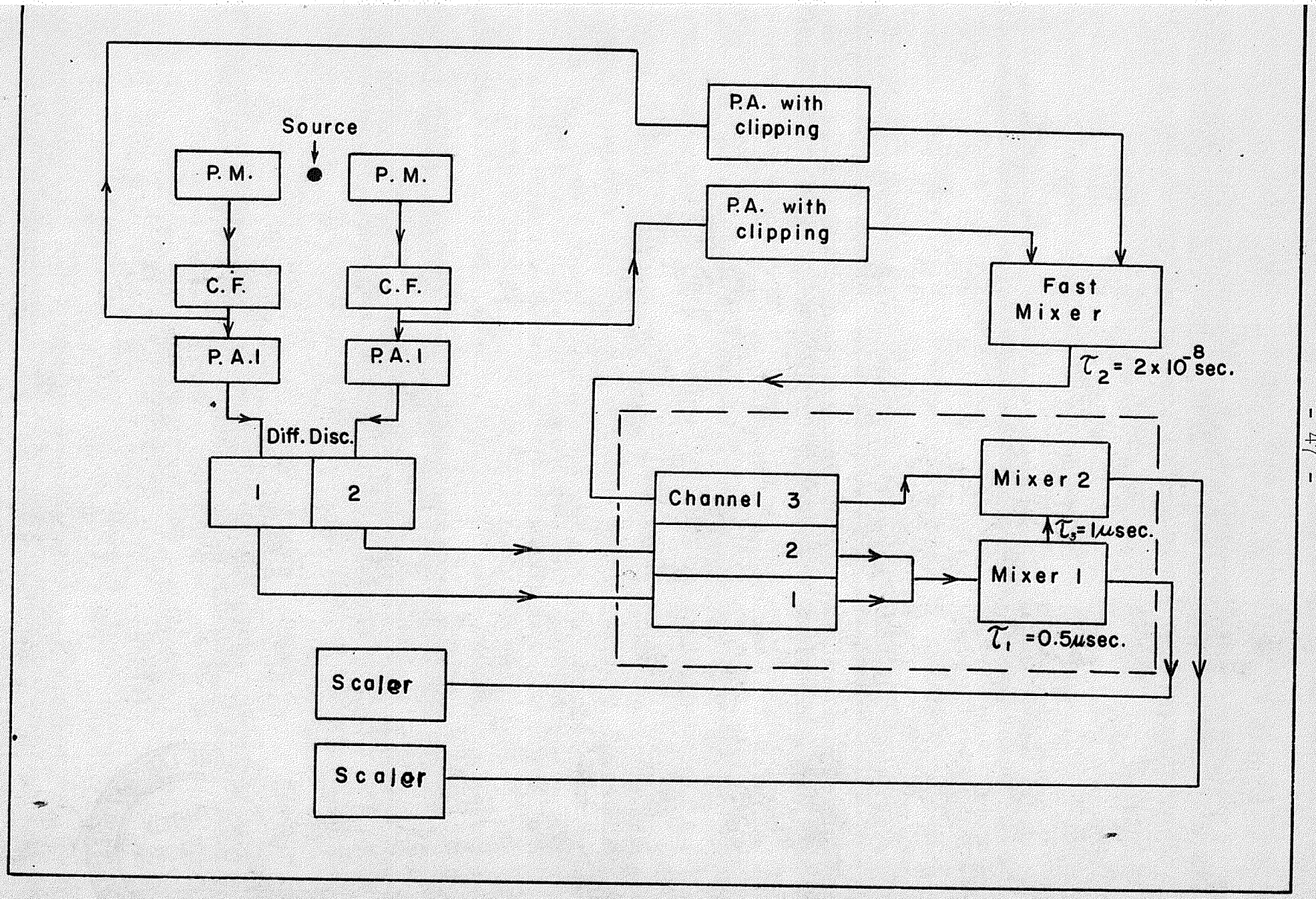

Diagram of the Fast-Slow Coincidence Circuit.

fed into channel 3 of the triple coincidence unit and coincidences are obtained in the second mixer between the output of the fast coincidence unit ($\tau = 2\text{x}10^{-8}$ sec.) and that of the first mixer or slow coincidence unit ($\tau = 0.5\text{x}10^{-6}$ sec.). Of course the delay in channel 3 must be adjusted to account for the delay in channels 1 and 2 due to discrimination and mixing. The ratio of genuine coincidences to accidentals in the slow unit is given by equation (2.7) with $\tau = \tau_1 = 0.5\text{x}10^{-6}$ sec., i.e.

$$R_s = \left[\frac{N_c}{N_{12}^A}\right]_{\tau_1} = \frac{W(\theta)}{2N\tau_1}$$

This ratio for the fast-slow system is given by equation (2.7) also since the fast-slow system contains pulse-height discrimination with the resolving time determined by the fast mixer. Then for the fast-slow systems, $\tau = \tau_2$ and $R_{fs} = W(\theta)/2N\tau_2$. Since $W(\theta)$ and N are constant for given θ;

$$\frac{R_{fs}}{R_s} = \frac{\tau_1}{\tau_2} \quad \text{or} \quad R_{fs} = \frac{\tau_1}{\tau_2} R_s \ .$$

Now $\tau_1 = 5\text{x}10^{-7}$ sec. and $\tau_2 = 2\text{x}10^{-8}$. Therefore $R_{fs} = \frac{5\text{x}10^{-7}}{2\text{x}10^{-8}} R_s = 25\ R_s$. Thus the coincidence ratio for the fast system is 25 times as high as that for the slow system. Hence it can be seen why the fast-slow system has its merits over a simple slow system.

There are however, certain disadvantages about the fast unit that do not exist in the slow unit. One can obtain coincidences between pulses in the slow unit no matter how much they may differ in pulse height; thus if g_1 gives a pulse 2 volts high and g_2 a pulse 30 volts, because of the pulse shaping that takes place in the discriminators and in channels 1 and 2 the mixer still receives pulses from each channel of the same amplitude. This is no longer true for the fast system used in this investigation in which there is no pulse amplitude equalization. Thus a fast mixer sees pulses of unequal size and the best it can handle is a pulse height ratio of 2 to 1. It is most efficient with a pulse height ratio of 1 to 1. This meant that W^{182} could not be studied at all by the fast-slow system since the pulse height ratio for the gamma-rays studied was 18 to 1. The slow system was used for that case. Ni^{60} and Sm^{152} were studied successfully with the fast-slow system. With W^{182} the slow mixer was operated with a τ_1 of 10^{-7} seconds. Therefore $\frac{R_{fs}}{R_s} = \frac{10^{-7}}{2x10^{-8}} = 5$. Hence $R_{fs} = 5R_s$ and with the improved regulation and stability it was felt that the factor of 5 was not too serious a loss.

The Fischer and Marshall type coincidence unit was not the only fast unit tried. A high speed coincidence circuit which was designed by Z. Bay (26) was tried; however, the limitations of the apparatus prevented it from being used

successfully. The photomultipliers of this spectrometer are 10 stage with a gain of 10^7. Bay's circuit needs photomultipliers which have a gain of 10^9 or 14 stages. Even though his circuit is phenomenally fast (10^{-10} sec. resolving time) it can only operate with a pulse height ratio of 1 to 1, and at most 2 to 1. It was impossible to use this circuit on an isotope like W^{182} when the cascades of interest have a pulse height ratio of 18 to 1. In order to obtain a pulse height ratio of 1 to 1 the voltage of the photomultiplier which was detecting the low energy gamma was raised, but this only caused the photomultiplier to block so badly that the line could no longer be resolved. This, plus the fact that an extremely stable high gain amplifier was needed to amplify the output pulses from the coincidence circuit led the author to abandon any further attempts in this direction and to use the Fischer and Marshall type unit.

(c) Calibration of the Spectrometer

It is a well-known fact that the scintillation spectrometer exhibits a direct proportionality between pulse height and gamma-ray energy. Hence if the energy of an unknown gamma-ray is to be determined, one compares the pulse height due to its photoelectron line with that of a gamma-ray of known energy. If possible one uses mono-energetic gamma-rays for the calibration of the pulse height axis in energy units; two such sources which are suitable for this are Cs^{137} and Zn^{65}. Ni^{60} can also be used because it has two gamma-rays that can be resolved distinctly. A full treatment of the spectrometer calibration methods is contained in the literature (24,27).

The theory of Angular Resolution measurements was presented in Section (c) of Chapter I. The experimental techniques used to obtain the necessary resolution curves will now be described. The method of Lawson and Frauenfelder (12) was used for all energies except for those energies near 0.511 mev where the method of Church and Kraushaar (17) was used. Figure 4 illustrates the collimating system used. The beam is parallel to the axis of the fixed detector and analyzed by the movable detector. The source to crystal distance in an experiment using a gamma-ray of a certain energy was the same as the distance AO in measuring the angular resolution curve for that energy. Spectrometer no. 2 was used for these measurements. The spectrum was scanned with the differential discriminator and the gate set

over the photoelectron line to be examined. The detector was moved in 2.5° increments from 145° to 215° with the counting rate being recorded for each position. The counting rate, corrected for background was plotted against the angle that counter 2 (movable counter) made with counter 1 (fixed counter). The angular resolution curves for the following gamma-ray energies were measured:

(a) 67.4 kev photoelectron line in W^{182}

(b) 312 kev photoelectron line in Ir^{192}

(c) Annihilation radiation from Zn^{65}

(d) 1172 kev photoelectron line in Ni^{60}

(e) 1332 kev photoelectron line in Ni^{60} .

The angular resolution curves for the 1172 kev and the 1332 kev lines in Ni^{60} were measured for two reasons. The first being that they were needed for calibration purposes for the angular correlation measurements of Ni^{60}. The second being that the angular resolution curve for the 1172 kev line in Ni^{60} could be used to calibrate the equipment for both the 1222 kev and the 1122 kev line in W^{182}.

The 67.4 kev line in W^{182}, which is very intense, was used for its own angular resolution curve.

Taylor (28) mentions that the background in the laboratory was comparable in magnitude to the beam intensity for the lower energy gamma rays (312 kev and 662 kev) in Ir^{192}. This difficulty was overcome by using a stronger W^{182} source (Taylor used 10 microcuries of Ir^{192}, the author 20 microcuries of W^{182}). The angular

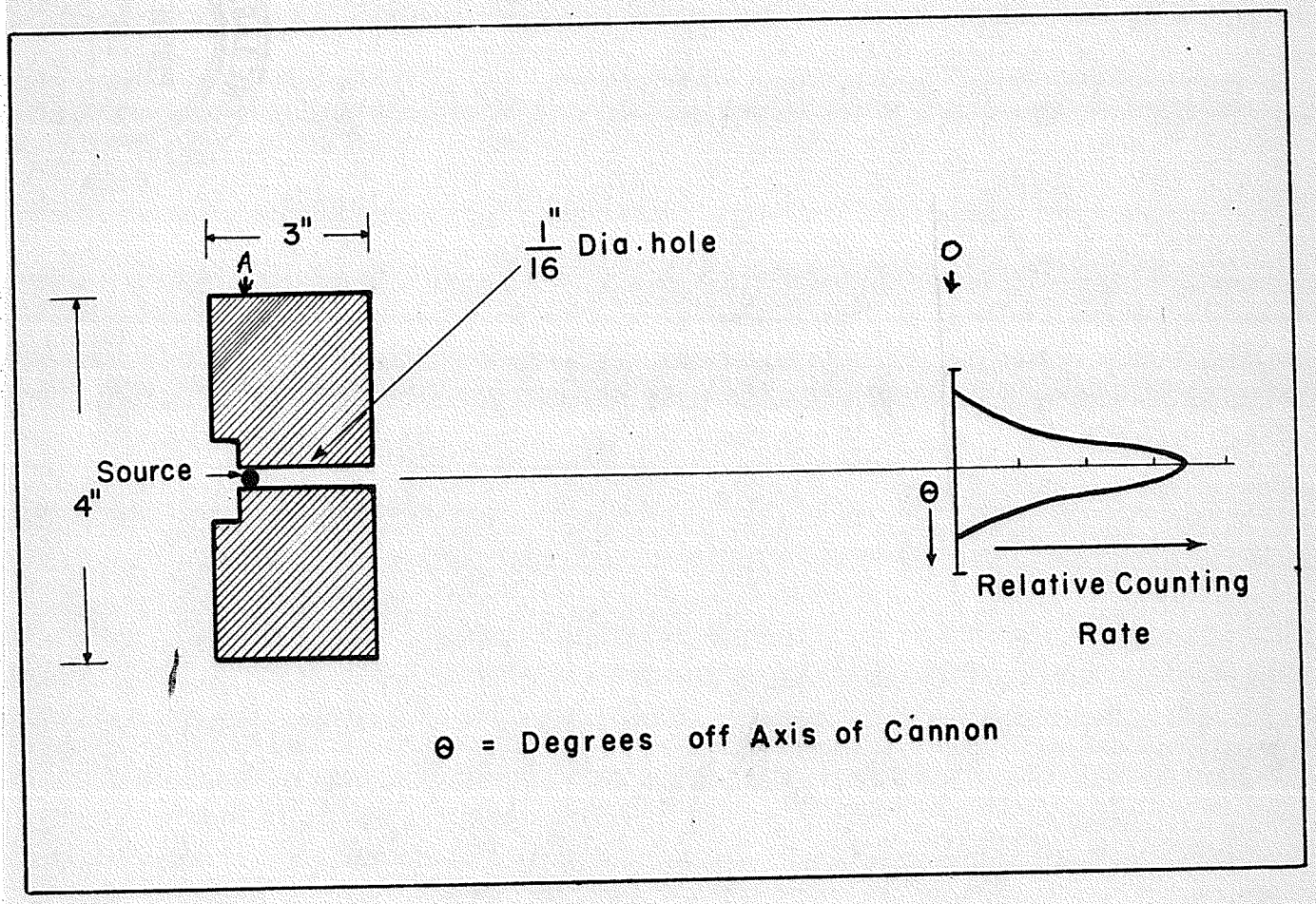

Fig. 4. Collimating system and shape of gamma-ray beam used for the determination of the angular resolution of the scintillation counters.

resolution curves for gamma-rays (b), (c) and (e) are in substantial agreement with those of Taylor and hence were not reproduced. The angular resolution curves for gamma-rays (a) and (b) are reproduced in Figs. 5(a) and 5(b).

The J_{2k} of equation (1.45) were evaluated with a planimeter. The results along with the gamma-ray energies used are tabulated in Table I. Since both counters never detected radiations of the same energy, only the ratios J_2/J_o, J_4/J_o were recorded. The Q_2/Q_o and Q_4/Q_o must be evaluated from (1.44) since each counter detected only one gamma-ray of a given energy.

Another point worth mentioning is the calibration of the spectrometer with regard to delays. The delays of each channel are energy dependent, and the delays between the various channels should be adjusted for maximum coincidences for each pair of energies studied. The author found that a delay setting for one cascade, say the 1172 → 1332 kev cascade in Ni^{60} would be quite different from the low energy cascade 122 → 244 kev in Sm^{152}.

Table I

Gamma-Ray Energy		Source	$\frac{J_2}{J_o}$	$\frac{J_4}{J_o}$
a	67.4 kev	W^{182}	0.941	0.832
b	312 kev	Ir^{192}	0.942	0.833
c	511 kev	β^+-Zn^{65}	0.957	0.865
d	1172 kev	Ni^{60}	0.950	0.825
e	1332 kev	Ni^{60}	0.942	0.852

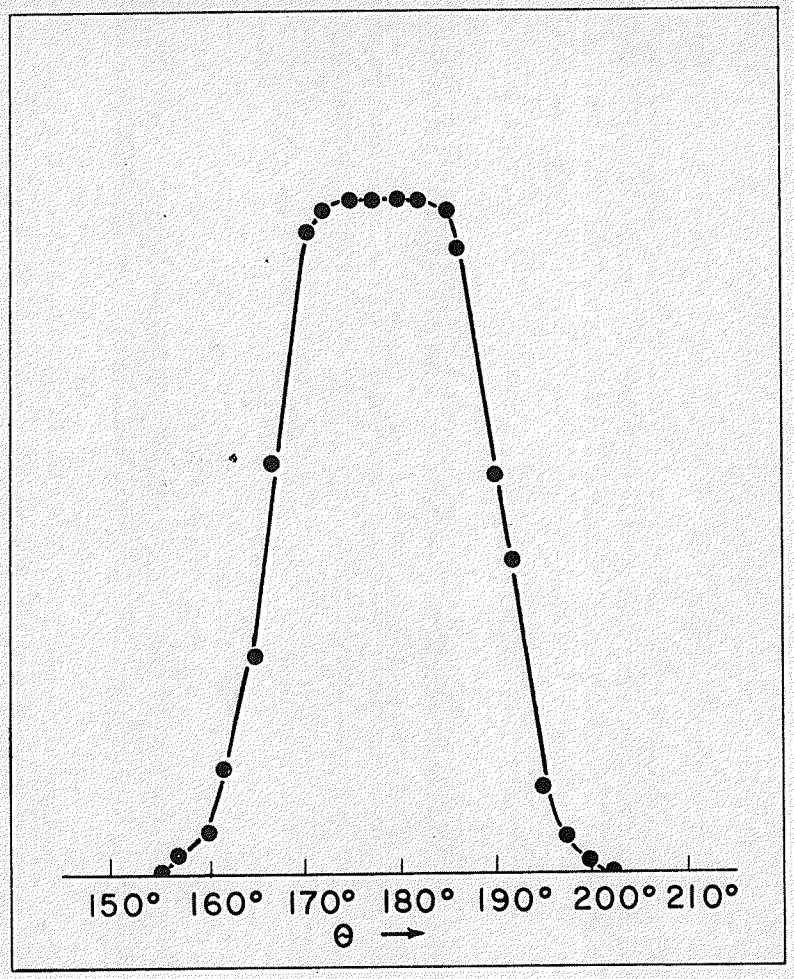

Fig. 5(a) Angular resolution curve for the 67.4 photoelectron line in W^{182}.

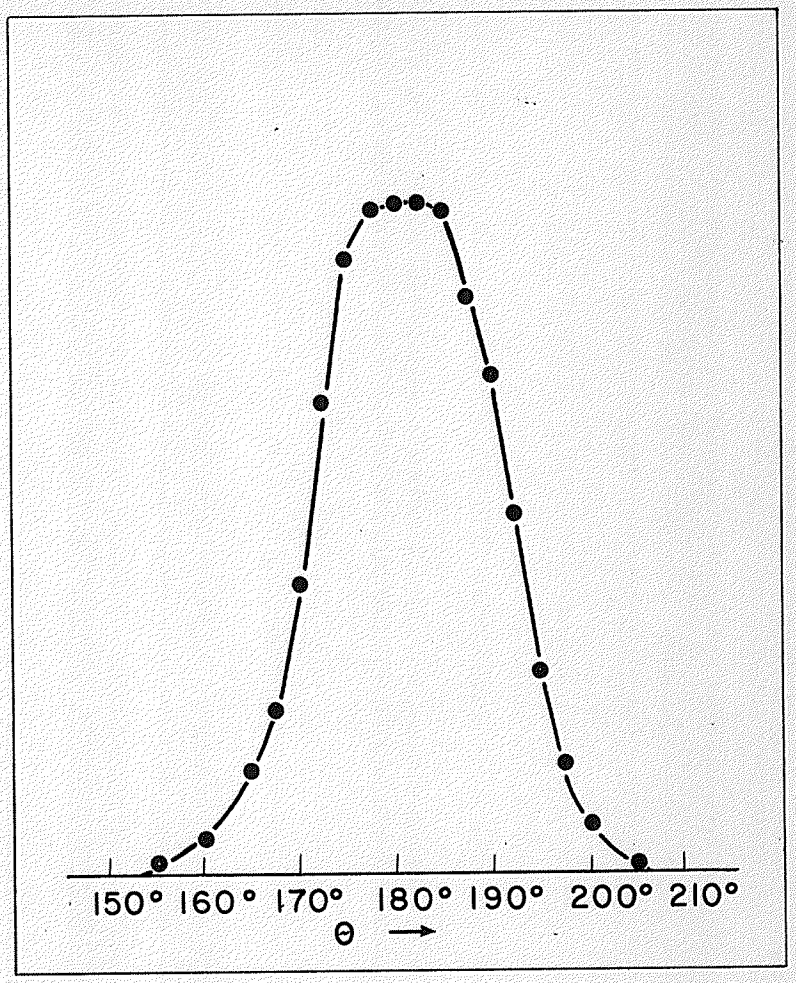

Fig. 5(b) Angular resolution curve for the 1172 kev line in Ni^{60}.

Chapter III

Experimental Results

(a) Application of the fast-slow coincidence spectrometer to Ni^{60}

Ni^{60} is an even-even nucleus that is well suited for angular correlation measurements. It has prominent photoelectron peaks for the cascade of interest, i.e. the 1172 → 1332 kev cascade. Even-even nuclei are supposed to have spin zero in their ground state which means that the second transition $j(g_2)0$ is pure. Ni^{60} has been the basis of many investigations. (2,10,12,24,29,30,31). A good introductory discussion is also given by H. Frauenfelder in Siegbahn's Beta and Gamma-Ray Spectroscopy. Because of the wealth of literature that exists on the angular correlation in Ni^{60}, the author will restrict his discussion to the accuracy of the measurements made on Ni^{60} with the fast-slow system.

The pulse-height ratio of the 1172 → 1332 kev cascade is 1.116, hence the 6BN6 coincidence unit was usable for this cascade. The source was a small metallic pellet of Co^{60} with a strength of 0.1 millicurie, supplied by Atomic Energy of Canada Limited. The spectrum of Ni^{60} was obtained with each channel, whereupon the gates of the differential discriminators were widened and set over their respective photopeaks. The correlation was first studied with the slow system with a resolving time of 10^{-7} seconds. The genuine to accidental coincidence

ratio for this isotope was 2.5 to 1. Counting intervals of 40 minutes were used. The measurements were taken at five different values of θ; 90°, 120°, 140°, 160° and 180°. As mentioned in Chapter I, Section (d), the singles, coincidence and accidental rates were taken at each position. Each reading was repeated three times and the mean taken. The singles counting rate varied by less than 1% over the five positions.

The experiment was then repeated with the fast-slow apparatus, which has a resolving time of 2×10^{-8} seconds. Theory says the coincidence ratios for the two systems should be

$$\frac{R_{fs}}{R_s} = \frac{\tau_1}{\tau_2} = \frac{10^{-7}}{2\times10^{-8}} = 5.$$

Hence $R_{fs} = 5R_s$. The accidentals dropped to 2 every 5 minutes where there were 10 every five minutes previously. The genuine to accidental ratio ~~per five minute interval~~ was 12.0 to 1 rather than the 12.5 to 1 that was to be expected theoretically. The percentage difference between these two coincidence ratios, i.e. actual and theoretical coincidence ratios, is 4%. This means that even with a pulse-height ratio of 1.116, a few coincidences are missed.

A function of the form

$$W(\theta) = \sum_k A_{2k} P_{2k}(\cos\theta) = \sum_k a_{2k} \cos^{2k}\theta$$

was fitted to the experimental points using the methods of least squares. The coefficients A_{2k} and a_{2k} were then corrected for the finite angular resolution of the detectors. The net correction factors were $Q_2/Q_o = 0.895$, $Q_4/Q_o = 0.703$ since each counter detected one gamma-ray only.

The errors in these coefficients were found by the method outlined in Chapter I(b). It was pointed out in that section that the error in the anisotropy should be taken as the error in the experiment since the errors in the coefficients a_{2k} or A_{2k} contain the errors in the least squares fit.

Table II

	A_2	A_4	A(anisotropy)
Slow system	0.999±0.022	0.0089±0.004	0.163±0.006
Fast-slow System	0.101±0.004	0.0090±0.002	0.166±0.002
Theory	0.102	0.0091	0.1667

Table II consists of the corrected coefficients A_2 and A_4, the measured anisotropies and their associated errors. The error in the anisotropy, which will be taken as an estimate of the error in the correlation, is 1.2% for the fast-slow system and 3.6% for the slow system. This shows that the fast-slow system is capable of very high precision. It should be noted that even though this error seems small, it is not as small as the error reported by Steffen (32) which is 0.6%. The coefficients obtained by the method of least squares, after

correction, were found to yield the usual Ni^{60} assignment $4(E_2)2(E_2)0$. Since both radiations are quadrupole, the assignment of spin 2 to the first excited state and 4 to the second excited state follows. The electric character of the radiations indicates that there is no parity change in these transitions. The complete decay scheme with these assignments is shown in Fig. 6. Lloyd (33) has introduced the idea of basic 2^{L_1}-pole-2^{L_2}-pole gamma-gamma angular correlation. He found that the coefficients A_{2k} are the same for both of the 2^{L_1}-pole-2^{L_2}-pole cascades $j\text{-}L_1(L_1)j(L_2)j+L_2$ and $j+L_1(L_1)j(L_2)j\text{-}L_2$; furthermore, the coefficients A_{2k} for these particular cascades are independent of j, i.e. they are not dependent on the spins of the initial, intermediate and final nuclear states, only on the multipolarity of the radiations. Transitions of this type are called basic. Evidently the Ni^{60} 1172 → 1332 kev cascade is a basic 2^2-2^2 correlation. Lloyd's tables are very useful for fast identification of the coefficients A_{2k}. Fig. 7 shows the plot of the uncorrected curves for the fast-slow and the slow system. Notice that there is a slight scatter to the points belonging to the slow system in comparison to those of the fast. With the usefulness of the fast-slow system established it was used to study Sm^{152}.

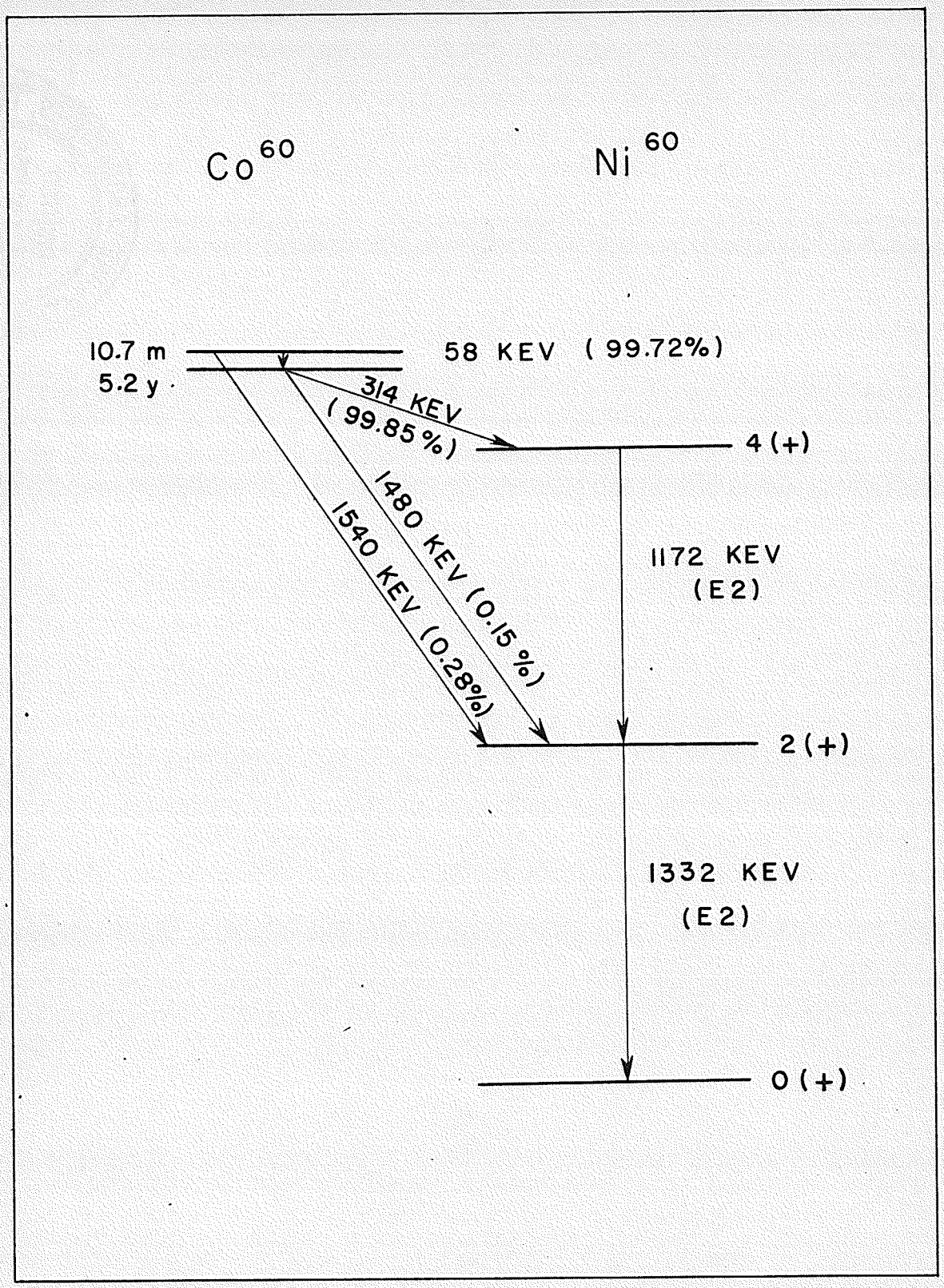

Fig. 6 Decay Scheme of Co^{60} (Taken from Keister and Schmidt, Phys. Rev. 93(1954)140).

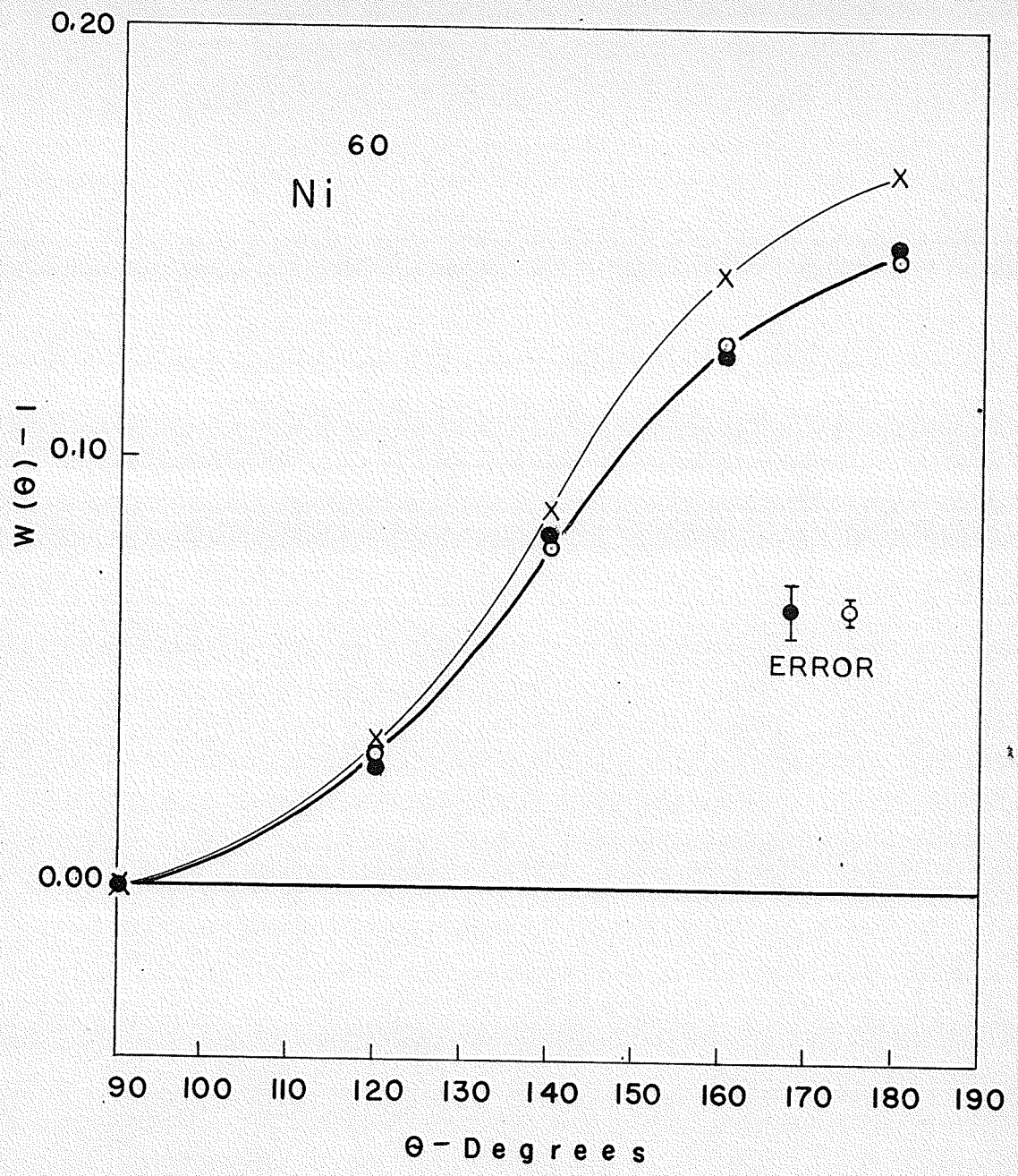

Fig. 7. Directional correlation function for the 1772 → 1332 kev cascade in Ni^{60}. The lower curve is the uncorrected least squares fit to the experimental points. The black dots belong to the slow-coincidence system while the white dots belong to the fast-slow system. The crosses are the Theoretical points for a $4(E_2)2(E_2)0$ assignment. The magnitudes of the error on the black and white dots are shown on the right hand side. The corrected curve (not shown) follows a $4(E_2)2(E_2)0$ assignment.

(b) Directional Correlation in W^{182}

(i) Properties of W^{182}

The isotope Ta^{182} decays by beta-minus emission into excited states of W^{182} which is one of several complex gamma-emitting nuclei of even-even species. The decay scheme of W^{182}, containing some twenty-seven gamma-rays, has been subject to a number of investigations (34,35,37,38).

Four of these investigations (34,35,37,38) were concerned with energy determinations of the gamma-radiation using curved crystal gamma-ray diffraction spectrometers and beta-ray spectrometers. Mihelich (36) performed a coincidence experiment which determined the order of some of the lower levels in W^{182}. The most recent of these investigations, performed by Murray, Boehm, Marmier and Dumond (38) was quite successful in that it succeeded in measuring the energies and relative intensities of gamma-rays and conversion lines arising from 27 transitions in W^{182}. They deduced the internal conversion coefficients and multipolarities for most of the transitions which together with the gamma-ray energies formed the basis of their proposed decay scheme for W^{182} (Fig. 8).

The measurement of the gamma-ray energies with the curved crystal spectrometer enabled them to identify most of the conversion lines observed with the beta-ray spectrometer. Their internal conversion coefficients were obtained from the combination of gamma-ray and conversion line intensities. Their multipolarity assignments were made largely on the basis of the

comparison of observed and theoretical (39,40) k-and L-shell internal conversion coefficients. In several cases their comparisons were ambiguous requiring additional arguments.

They do admit that level I (Fig. 8) is very uncertain. They also state that the energies of levels E through K are more certain relative to level D than to the ground state since their connection to the ground state involves only high-energy transitions with rather large uncertainties. Their spin assignments for levels B and C are definite while that for level D may be questionable because of the uncertainties in the conversion data for transitions DA and DB. They have pointed out that for the levels above D there are many possible sets of spin assignments compatible with their multipolarities of the transitions. Their proposed assignment, although reasonable is largely speculative for levels D and those above it.

The author undertook to ascertain the spin assignments of levels D, F and H because they are connected by the following gamma-ray cascades:

(1) The 67.74 → 1222 kev cascade, i.e. F → D → A.

(2) The 152.4 → 1222 kev cascade, i.e. H → D → A.

(3) The 67.74 → 1122 kev cascade, i.e. F → D → B.

Mihelich (36) has shown from his coincidence work that the 1122 kev gamma-ray is a transition between levels D and B while the 1222 kev gamma is a transition between D and A. The work of Murray et al (38) agrees with that of Fowler et al (35)

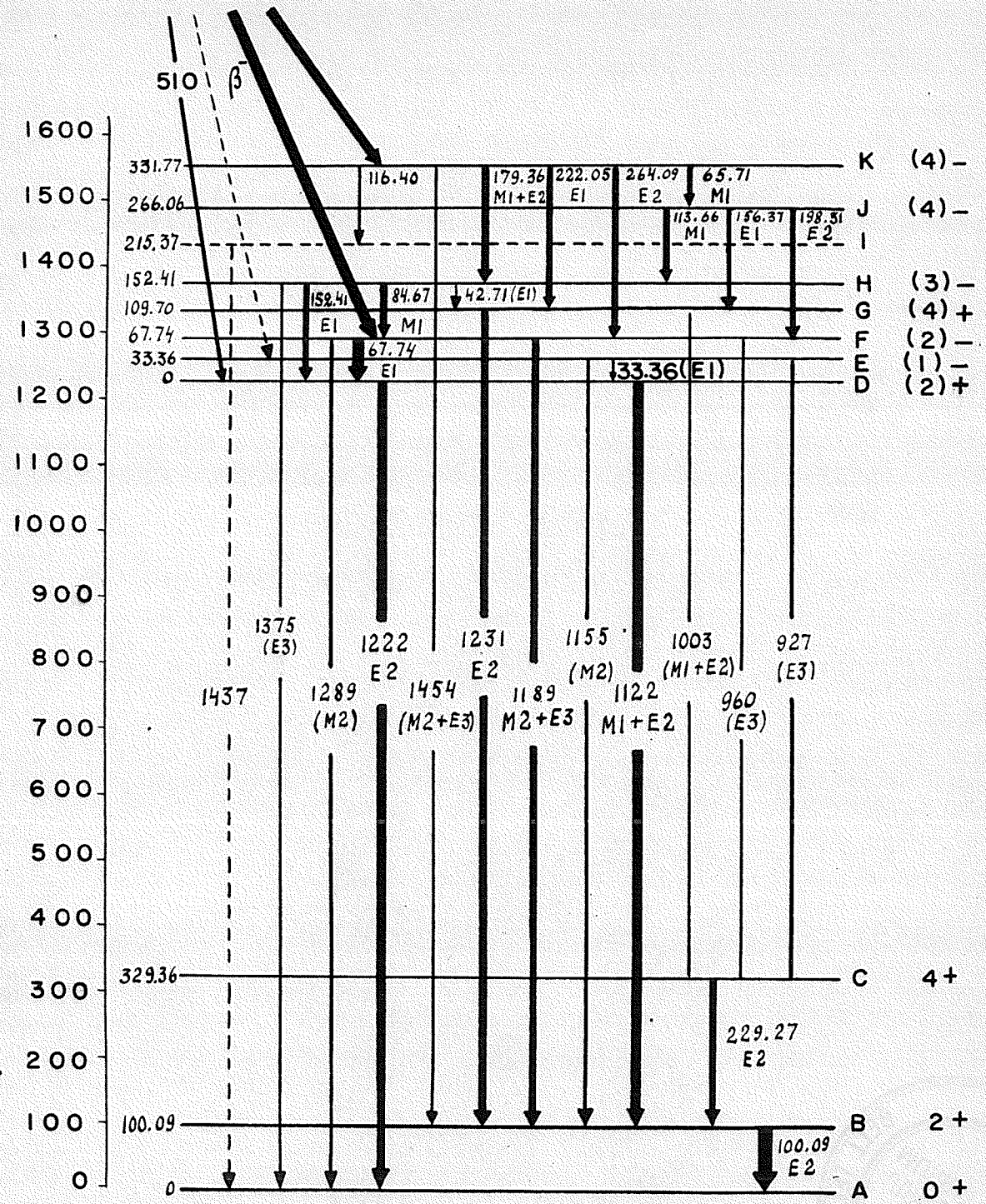

Fig. 8. Energy levels in W^{182}. Taken from Murray et al (44).

for the spin assignments of levels A, B and C but disagrees for the assignments of levels D to K. Both these authors have found that the assignments of levels A, B and C are in agreement with the Bohr-Mottelson theory (41).

(ii) Procedure

Taylor (46) tried to study the gamma-ray cascades (1) and (3) in W^{182} with his slow two-channel spectrometer without success. His coincidence ratio was 0.6 (32 counts per minute of which 20 were accidental) which means that it was impossible to obtain valid results. The lowest ratio that one can work with in directional correlation is unity, and for accurate results it should be at least 5.

The source was obtained from the Chalk River pile where it was prepared by irradiation of pure tantalum metal with slow neutrons. The reaction was Ta^{181} (n,γ) Ta^{182}. The source, of strength 20 microcuries was a spherical pellet 1/8" in diameter, 278 milligrams in weight.

W^{182} was studied with the slow two-channel system with a resolving time of 10^{-7} seconds. It could not be studied with the fast-slow system since the pulse height ratios for cascades (1), (2) and (3) are approximately 18 to 1, 8 to 1 and 17 to 1 respectively. The fast coincidence mixer will not operate with a pulse height ratio greater than about 2 to 1. However, the Hamner power supply N-401 and the Sorenson regulator stabilized the equipment to such an extent that the lowest coincidence ratio obtained was 4 to 1. The best coincidence ratio obtained was

7 to 1 with cascades (1) and (3). The counting rate for this case was approximately 8 every minute of which 1 was accidental.

The same technique was used in obtaining the correlation data for W^{182} that was used with the slow system on Ni^{60}. The singles counting rate varied by less than 1% over the five positions and counting intervals of 40 minutes were used, each reading was repeated six times for all three cascades. The bulk spectrum of W^{182} is shown in Fig. 9. The intensities of the gamma-rays studied are shown in Table III, these values being taken from Murray et al (38).

Table III

Gamma-ray energy (kev)	Gamma-ray intensity
67.74	85
152.41	35
1122.0	100
1222.0	95

(iii) Spin and Multipolarity Assignment

The 67.4 → 1222 kev cascade (F → D → A) will be discussed first. The 1222 kev transition (D → A) is a transition to a ground state with a spin of zero. When a transition from a level of spin j to the ground state ($j_2 = 0$) takes place only those transitions are allowed which have the multipolarity of the radiation equal to the spin of the excited state in question,

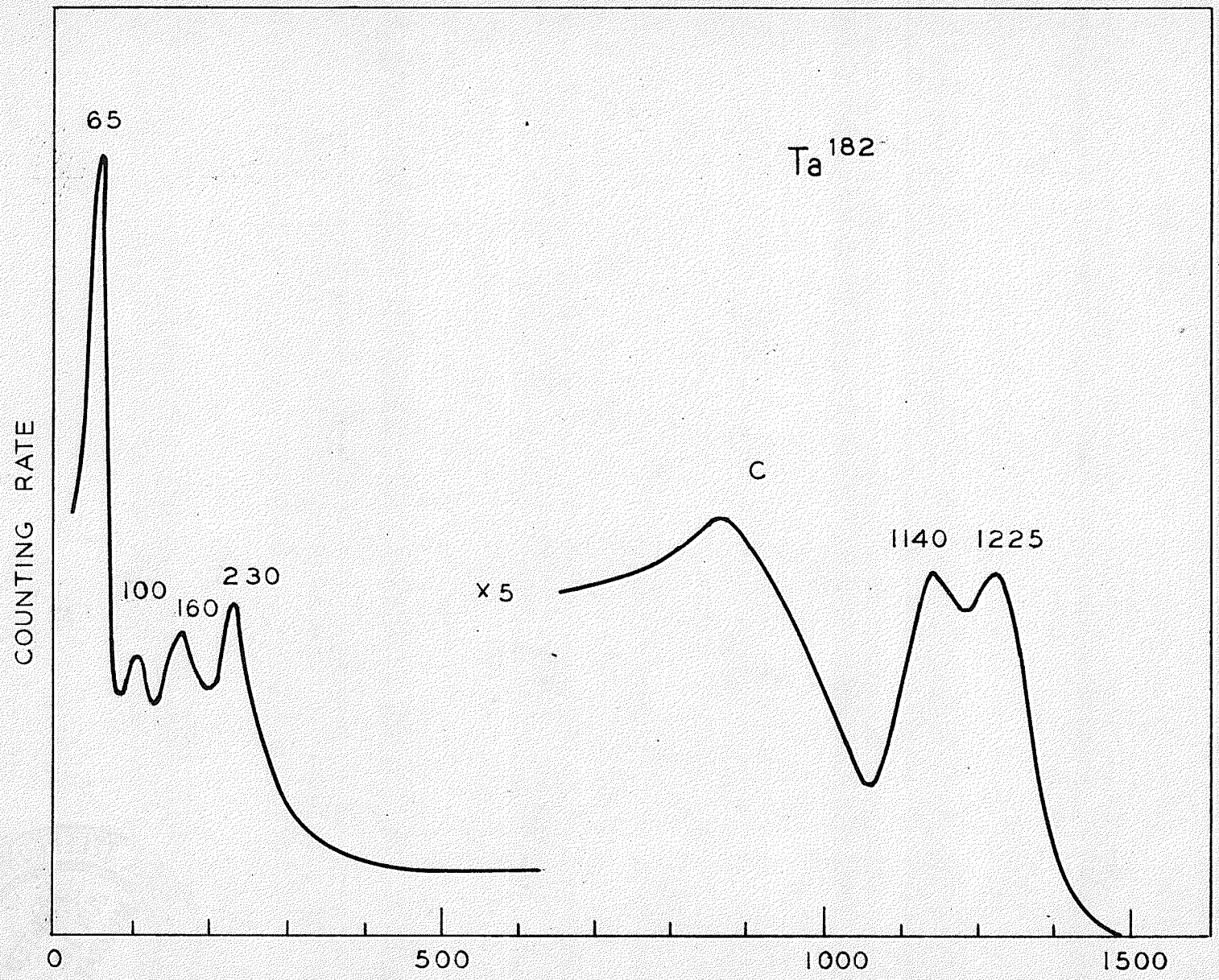

Fig. 9. Gamma-ray spectrum of W^{182} following beta-minus emission in Ta^{182}.

i.e., $j(L_2)j_2 = j(L_2=j)0$. This follows from the selection rules (60) used in gamma-gamma angular correlation work:

$$| j_1-j | = L_1 \text{ if } j_1 \neq j \text{ however if } j_1 = j \text{ then } L_1 = 1 \text{ only} \quad (3.1)$$

$$| j_2-j | = L_2 \text{ if } j_2 \neq j \text{ however if } j_2 = j \text{ then } L_2 = 1 \text{ only.} \quad (3.2)$$

Since the ground state has spin zero ($j_2=0$) the selection rule (3.2) says the only allowed transitions are those with $| j | = L_2$, i.e. the radiation multipolarity must equal the spin of the excited state in question.

Thus the only spin sequences allowed for the 1222 kev transition are of the type $j(L_2=j)0$. The values of j can run through all integers starting at 1. Since the radiation multipolarity must equal the spin of the level j one can ask what multipolarities are allowed and hence determine what spins are allowed. Gamma-gamma directional correlation experiments have never observed radiations with an $L > 2$. (61) The only multipolarities observed in experiments of this type are dipole or quadrupole. Hence one can insist that the allowed spin sequences for the 1222 kev transition be $j(L_2=j)0$ with $L_2 \leq 2$. Thus the spin j is either 1 or 2 depending upon whether the radiation is either dipole or quadrupole. The spin sequences that can describe the 67.4 → 1222 kev cascade will be of the type $j_1(L_1)1(1)0$ or $j_1(L_1)2(2)0$. These sequences along with the corresponding theoretical values of the angular correlation

coefficients are listed in Table IV. The multipolarity L_1 of the 67.4 kev gamma-ray is assumed to be either 1 or 2 leading to 12 different possible spin sequences. These sequences were arrived at by application of the angular momentum selection rules (3.1).

Table IV

Theoretical Values of Coefficients		
Spin Sequence	A_2	A_4
1(1)1(1)0	-0.250	0
2(1)1(1)0	+0.0501	0
1(2)1(1)0	-0.250	0
2(2)1(1)0	+0.250	0
3(2)1(1)0	-0.0715	0
1(1)2(2)0	-0.2505	0
2(1)2(2)0	+0.250	0
3(1)2(2)0	-0.0714	0
1(2)2(2)0	+0.1788	0
2(2)2(2)0	-0.0766	+0.326
3(2)2(2)0	-0.202	-0.0816
4(2)2(2)0	+0.102	+0.0091

Murray et al (38) have shown by measuring the conversion lines and gamma-ray energies in W^{182} that the 1222 kev gamma-ray is E_2. Thus all spin sequences of the type $j_1(L_1)1(1)0$ are ruled out

and one need only consider the seven spin sequences of the type $j_1(L_1)2(2)0$.

The theoretical angular correlation coefficients of these seven spin sequences will be compared with those coefficients obtained experimentally with the slow system. The particular spin sequence whose theoretical coefficients agree with the experimental coefficients will yield the spin assignment for the 67.4 → 1222 kev cascade. Table V shows the angular correlation coefficients obtained from a least squares fit of the data.

Table V

Angular Correlation Coefficients for the 67.4 → 1222 kev Cascade in W^{182}

Uncorrected		Corrected		Theoretical: 2(1)2(2)0	
a_2'	A_2'	a_2	A_2	a_2	A_2
0.3965	0.2335	0.450	0.261	0.428	0.250

The correlation function for the 67.4 → 1222 kev cascade is then given by:

$$W(\theta)-1 = + (0.261 \pm 0.095)P_2(\cos\theta). \qquad (3.3)$$

A graph of the corrected (equation 3.3) and uncorrected least squares fit is shown in Figure 10. This corresponds to a spin assignment of 2(1)2(2)0. The error in the coefficient

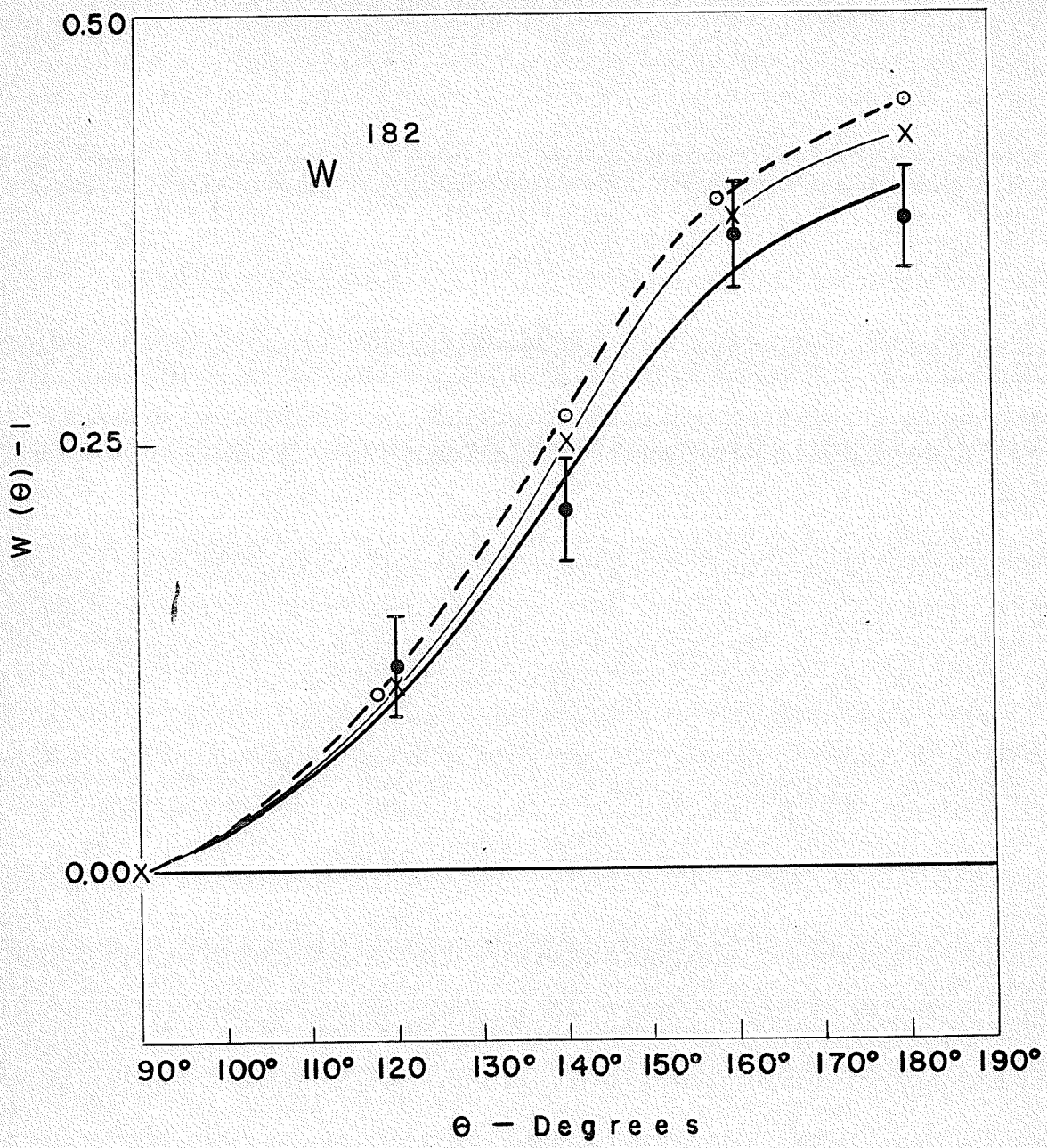

Fig. 10. Directional correlation curves for the 67.74 → 1222 kev gamma-ray cascade in W^{182} obtained with the slow system. The lowest curve is $W(\theta)-1=0.2335P_2(\cos\theta)$ which is the least squares fit to the experimental points (black dots). The crosses are the theoretical points for a $2(E_1)2(E_2)0$ assignment. The dashed curve with white dots is $W(\theta)-1=0.2611P_2(\cos\theta)$ which is the least squares fit corrected for finite angular resolution.

$$A_2 = + (0.261 \pm 0.095)$$

is large, but the error in the anisotropy is much less being of the order of twelve percent, i.e.,

$$A = + (0.450 \pm 0.054).$$

This agrees well with the theoretical anisotropy $A = + 0.4286$ of the 2(1)2(2)0 cascade.

If this assignment is examined from the point of view of the collective model of the nucleus one can draw some interesting conclusions. Assume that the Bohr-Mottelson theory applies to W^{182} in its simplest form, that is to say without K-forbiddenness (K is the projection of the total angular momentum of the nucleus on the nuclear symmetry axis). Then level D will have spin 8 because this model predicts the existence of a 677.6 kev level which would have spin 6. Evidence for a level at 680 kev is mentioned by Fowler et al (35). Level F will then have a spin of 12 and the spin sequence for the 67.4 → 1222 kev cascade would be 12 → 8 → 0. This assignment of course is completely impossible by virtue of the previous arguments.

Since the spin sequence is not 12 → 8 → 0 this means that the spectrum of W^{182} is not purely rotational. A purely rotational spectrum is predicted by the collective model for a separable nuclear wave equation, i.e. without K-forbiddenness. When K-forbiddenness is taken into account by this model its

predictions are in perfect agreement with the author's spin assignments. This point will be discussed later.

It can then be concluded that the 67.4 → 1222 kev cascade has the spin and multipolarity assignment 2(1)2(2)0. Both levels F and D then have spin 2. This agrees with the assignments of Murray et al (38).

The second cascade studied in W^{182} was the 152.4 → 1222 kev cascade. It has been shown that the 1222 kev transition has a 2(2)0 spin sequence. Thus the spin sequences that will describe the 152.4 → 1222 kev cascade will be of the type $j_1(L_1)2(2)0$. With the assumption that the 152.4 kev gamma is either dipole (L_1=1) or quadrupole (L_1=2) the selection rule (3.1) yields a total of seven spin sequences. These spin sequences along with the theoretical values of their angular correlation coefficients are the last seven sequences listed in Table IV.

The theoretical angular correlation coefficients of these seven spin sequences will be compared with those coefficients obtained experimentally with the slow system. The particular spin sequence whose theoretical coefficients agree with the experimental coefficients will yield the spin assignment for the 152.4 → 1222 kev cascade.

The angular correlation coefficients for the 152.4 → 1222 kev cascade are shown in Table V. These coefficients were obtained from a least squares fit to the experimental points.

Table V

Angular Correlation Coefficients for the 152.4 → 1222 kev Cascade in W^{182}

Uncorrected		Corrected		Theoretical: 3(1)2(2)0	
a_2'	A_2'	a_2	A_2	a_2	A_2
-0.077	-0.0527	-0.086	-0.059	-0.1035	-0.0714

Comparing the measured values of the angular correlation coefficients in their corrected form (Table V) with the theoretical values listed in Table IV shows that the 3(1)2(2)0 spin sequence fits the data for the 152.4 → 1222 kev cascade. The correlation function for this cascade is then:

$$W(\theta)-1 = -(0.059 \pm 0.025)P_2(\cos\theta). \qquad (3.4)$$

A graph of the corrected (equation 3.4) and uncorrected least squares fit is shown in Fig. 11. The error in A_2 is extremely large, i.e.

$$A_2 = -(0.059 \pm 0.025).$$

This is to be expected due to the low intensity of the 152.41 key transition, which reduces the ratio of genuine to accidentals to quite a low value, i.e. 4 to 1. The error in the anisotropy is not as high as the error in A_2, however. The anisotropy

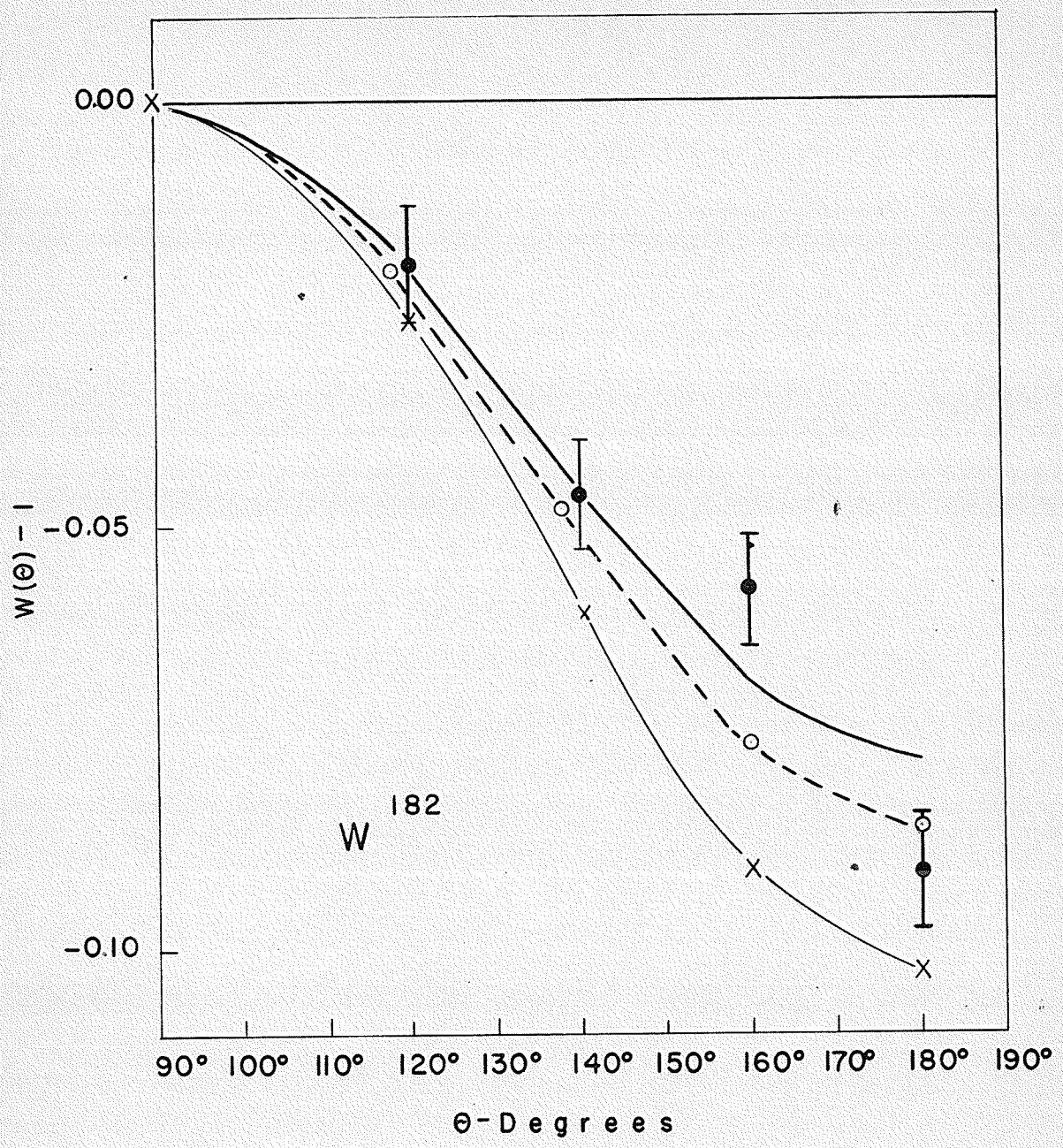

Fig. 11. Directional correlation curves for the 152.4 →1222 kev gamma-ray cascade in W^{182} obtained with the slow system. The highest curve is $W(\theta)-1=-0.0527P_2(\cos\theta)$: The least squares fit to the experimental points (black dots). The dashed curve with white dots is $W(\theta)-1=-0.049P_2(\cos\theta)$: The least squares fit corrected for finite angular resolution. The crosses are the theoretical points for a $3(E_1)2(E_2)0$ assignment.

$$A = -(0.086 \pm 0.018)$$

agrees reasonably well with the theoretical value A = -0.104. Further agreement is obtained with Murray et al (38) who indicate that the 152.4 kev transition is pure E_1. They had tentatively assigned spin 3 to level H. Thus to an uncertainty of 21% a spin of 3 is assigned to level H. The assignment of spin 2 to level D is much more certain because of the correlation of cascade (1).

The last cascade that will be discussed in W^{182} is the 67.4 → 1122 kev cascade. This cascade enables the spins of levels F and D to be checked and the mixing in the 1122 kev transition to be determined. The angular correlation coefficients for the 67.74 → 1122 kev cascade are shown in Table VI. These coefficients were obtained from a least squares fit to the experimental points.

Table VI

Angular Correlation Coefficients for the 67.4 → 1122 kev Cascade in W^{182}

Uncorrected		Corrected		Theoretical
a_2'	A_2'	a_2	A_2	These coefficients
-0.242	-0.1755	-0.268	-0.1963	are determined by δ.

The correlation function for this cascade is:

$$W(\theta)-1 = -(0.196 \pm 0.062)P_2(\cos\theta). \qquad (3.5)$$

A graph of the corrected (equation 3.5) and uncorrected least squares fit is shown in Figure 12. The analysis of equation (3.5) was performed by using equation (1.31). The functions W_I, W_{II} and W_{III} were calculated using the tables of Biedenharn and Rose (4).

Since the correlation of the 67.4 → 1222 kev cascade assigns spin 2 to both levels F and D and coulomb excitation experiments (44) along with internal conversion data (35,38) assign spin 2 to level B, the 67.74 → 1122 kev cascade was assigned the spin sequence 2 → 2 → 2 with the 67.74 kev transition being pure E_1 and the mixing in the 1122 kev transition to be determined by analysis. Murray et al (38) indicates that this transition has multipolarity $M_1 + E_2$. Assuming this to be the character of the radiation the functions W_I, W_{II} and W_{III} were found to be as listed in Table VII.

Table VII

Function	Spin Sequence
$W_I = 1 + 0.175\ P_2(\cos\theta)$	$j_1(L_1)\ j(L_2)\ j_2 \rightarrow 2(1)2(1)2$
$W_{II} = 1 - 0.0556\ P_2(\cos\theta)$	$j_1(L_1')\ j(L_2)\ j_2 \rightarrow 2(2)2(1)2$
$W_{III} = 0.2563\ P_2(\cos\theta)$	Interference between M_1 and E_2

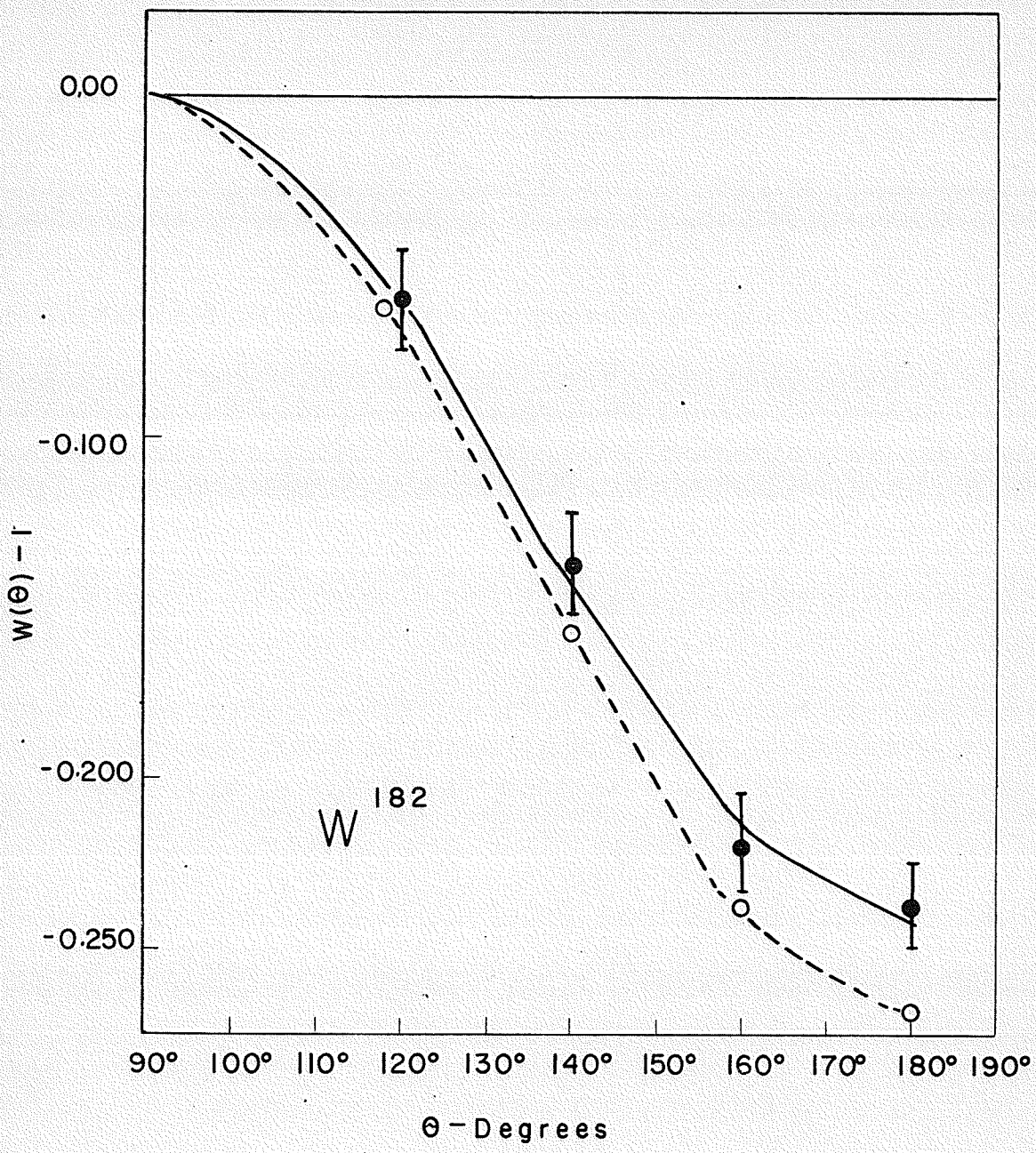

Fig. 12. Directional correlation curves for the 67.4 → 1122 kev gamma-ray cascade in W^{182} obtained with the slow system. The full curve is $W(\theta)-1=-0.1755P_2(\cos\theta)$: The least squares fit to the experimental points (black dots). The dashed curve with white dots is $W(\theta)-1=-0.1963P_2(\cos\theta)$: The least squares fit corrected for finite angular resolution. A $\delta=-3$ yields an assignment $2(E_1)2(90\%E_2 10\%M_1)2$.

Substituting these equations into equation (1.31) yields after normalization

$$W(\theta) - 1 = \left[\frac{0.175 + 0.5126\delta - 0.0536\delta^2}{1 + \delta^2}\right] P_2(\cos\theta). \qquad (3.6)$$

Thus $A_2 = \dfrac{0.175 + 0.5126\delta - 0.0536\delta^2}{1 + \delta^2}$. (3.7)

The Anisotropy $A = \left\{\dfrac{1 + A_2 + A_4}{1 - \frac{1}{2}A_2 + \frac{3}{8}A_4} - 1\right\}$ and

since $A_4 = 0$ $\qquad A = \dfrac{3A_2}{2-A_2}$. (3.8)

Substituting for A_2 yields

$$A = \frac{0.525 + 1.5378\delta - 0.1608\delta^2}{1.825 - 0.5126\delta + 2.0536\delta^2} . \qquad (3.9)$$

Figure 13 is a plot of A versus δ. The measured Anistropy is indicated by an arrow on the graph, its value is A =-0.268. This value corresponds to two values of δ, viz. $\delta = -3$ and $\delta = -1$. The choice of δ can be unambiguous by using internal conversion data. If $\delta = -3$ the mixture is 90% E_2 and 10% M_1. If $\delta = -1$ the mixture is 50% E_2 and 50% M_1. If $\delta = -3$ is correct the high percentage of E_2 should yield a K conversion coefficient of $\alpha_K = 5\times10^{-3}$. If $\delta = -1$ is correct the high percentage of M_1 should yield a K conversion coefficient of the order

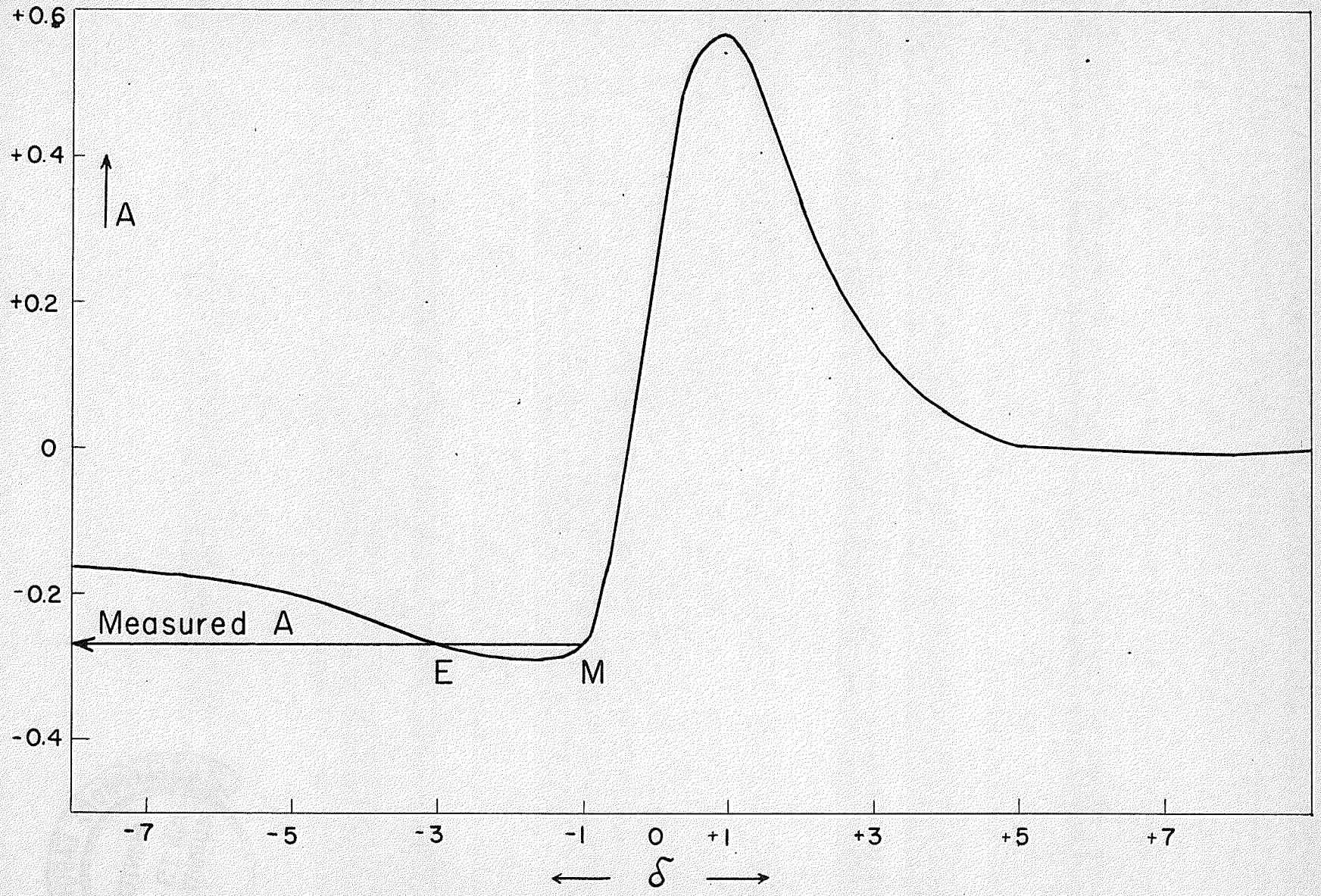

Fig. 13. Plot of the Anisotrophy A versus the intensity mixing ratio for the 67.4 → 1122 kev cascade in W^{182}.

of 10^{-2}. The measured K internal conversion coefficient (Murray et al (38)) of the 1122 kev line in W^{182} is $\alpha_K = 5 \times 10^{-3}$, thus $\delta = -3$. Hence the mixture in the 1122 kev line is 90% E_2 and 10% M_1 with a phase of 180° between the two radiations.

The assignments of spins 2, 2 and 3 to levels D, F and H respectively are in agreement with the theoretical assignments predicted by the collective model of the nucleus (47). Fig. 14 is the level scheme of W^{182} as predicted by the collective model of the nucleus. These reactions appear to populate states belonging to four different rotational bands. This is indicated by drawing members of the same bands (having same K and π) above each other, while the different bands are displaced sideways. The excitation energies are listed in kev and the states are labeled by the quantum numbers (K, j, π). The level scheme is interpreted as involving primarily states associated with four rotational series. The first series, comprising the three lowest levels, is the systematically occurring $K = 0+$ ground state rotational band of even-even nuclei. The calculated energy of the 6+ number of this band includes a small correction for the rotation-vibration interaction, as deduced from the observed energies of the 2+ and 4+ states. The second series beginning with the 1222 kev level has $K = 2+$ while the third series starts with the 1290 kev level with $K = 2-$. The beta-decay of Ta^{182} further populates a level at 1554 kev, which seems to be the lowest member of a fourth rotational band.

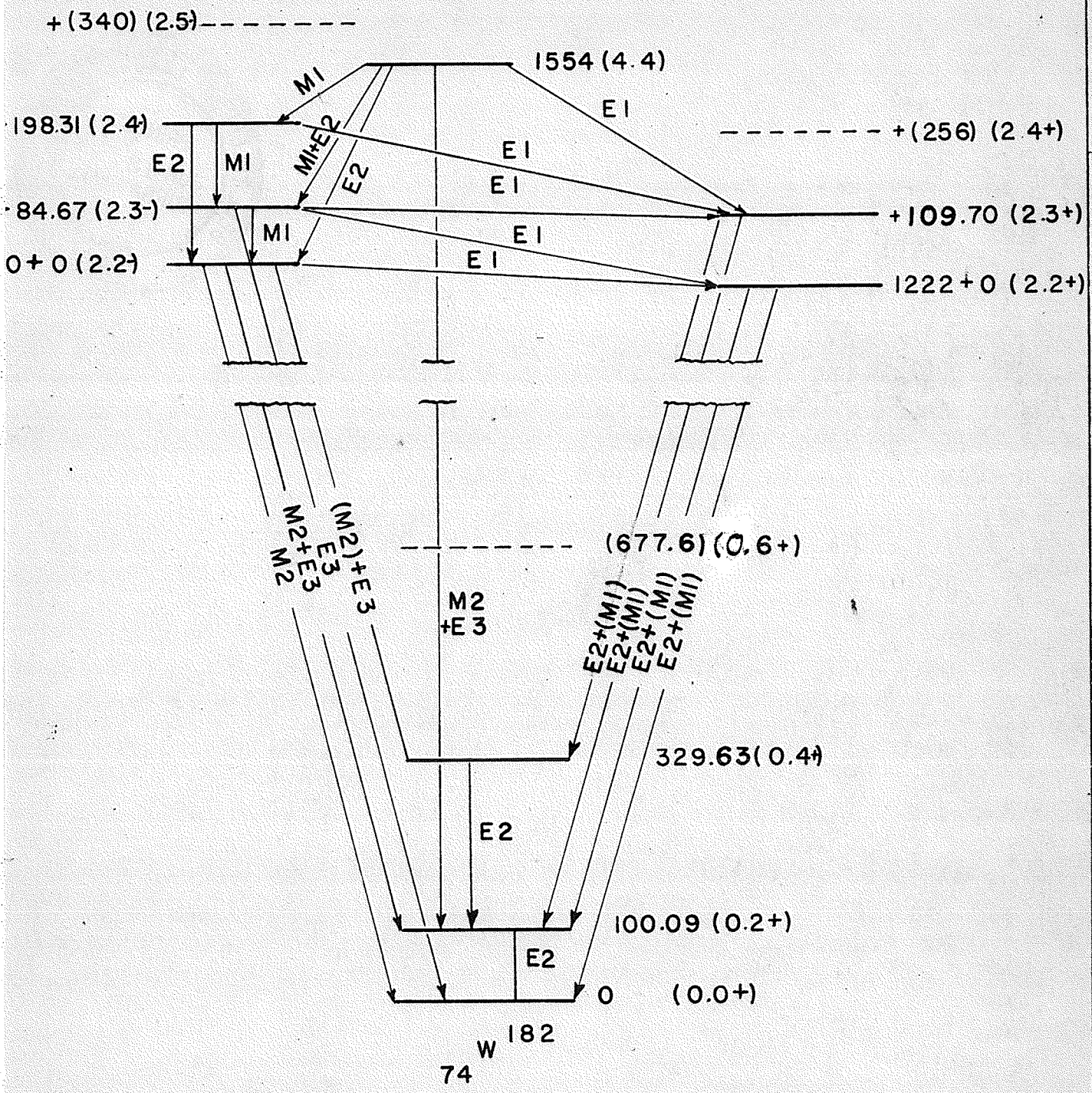

Fig. 14. Level Scheme of W^{182} as predicted by the Collective Model of the Nucleus. Taken from Alaga et al (57).

Thus it can be seen why the correlation yielded spin assignments of 2, 2 and 3 to levels D, F and H. Level D belongs to the second series (K = 2+) with spin j and parity π of 2(+). Levels F and H belong to the third series with j and π equal to 2(-) and 3(-) respectively. The 67.74 kev transition is a transition between the first state of the third series and the first state of the second series. The 152.41 kev transition is a transition between the second state of the third series and the first state of the second series. The high percentage of E_2 in the 1122 kev transition between levels D and B is due to the K-forbiddenness for M_1 radiation. Thus the collective model of the nucleus completely agrees with the experimental facts.

(c) Directional Correlation in Sm^{152}

(i) Properties of Sm^{152}

Eu^{152} has a half-life of 13 years and decays by K capture to Sm^{152} and by beta emission to Gd^{152}. Sm^{152} contains some eleven gamms-rays, six of which were recently identified by Grodzins (48). Since Sm^{152} has a Z of 62 it lies in the "strong coupling region" and can be classified as a strongly deformed nucleus. The decay of the long-lived $Eu^{152,154}$ mixture has been examined by many authors (48,49,50,51,52,53,54). These workers have identified at least two beta decays and many gamma transitions.

The source, obtained from Atomic Energy of Canada Limited, was produced by irradiation of Eu_2O_3 with neutrons ($Eu^{151}(n,\gamma)Eu^{152}$). Eu^{154} is also produced when Eu_2O_3 is irradiated but since the activity required of Eu^{152} was only 20 microcuries, the corresponding activity of Eu^{154} was very small, i.e. less than one microcurie. The target salt was sealed in an aluminum tube 1/4" by 1/8". The bulk spectrum of $Eu^{152,154}$ is shown in Figure 15. This was obtained with spectrometer No. 2. The decay scheme of Eu^{152} as proposed by Grodzins (48) is shown in Figure 16. The lines in Figure 15 that are identified are probably composite to some extent. Since some of the lines found by Grodzins are fairly weak and very close in energy to each other the resolution of spectrometer No. 2 would not be good enough to resolve them. In the decay scheme of Figure 15

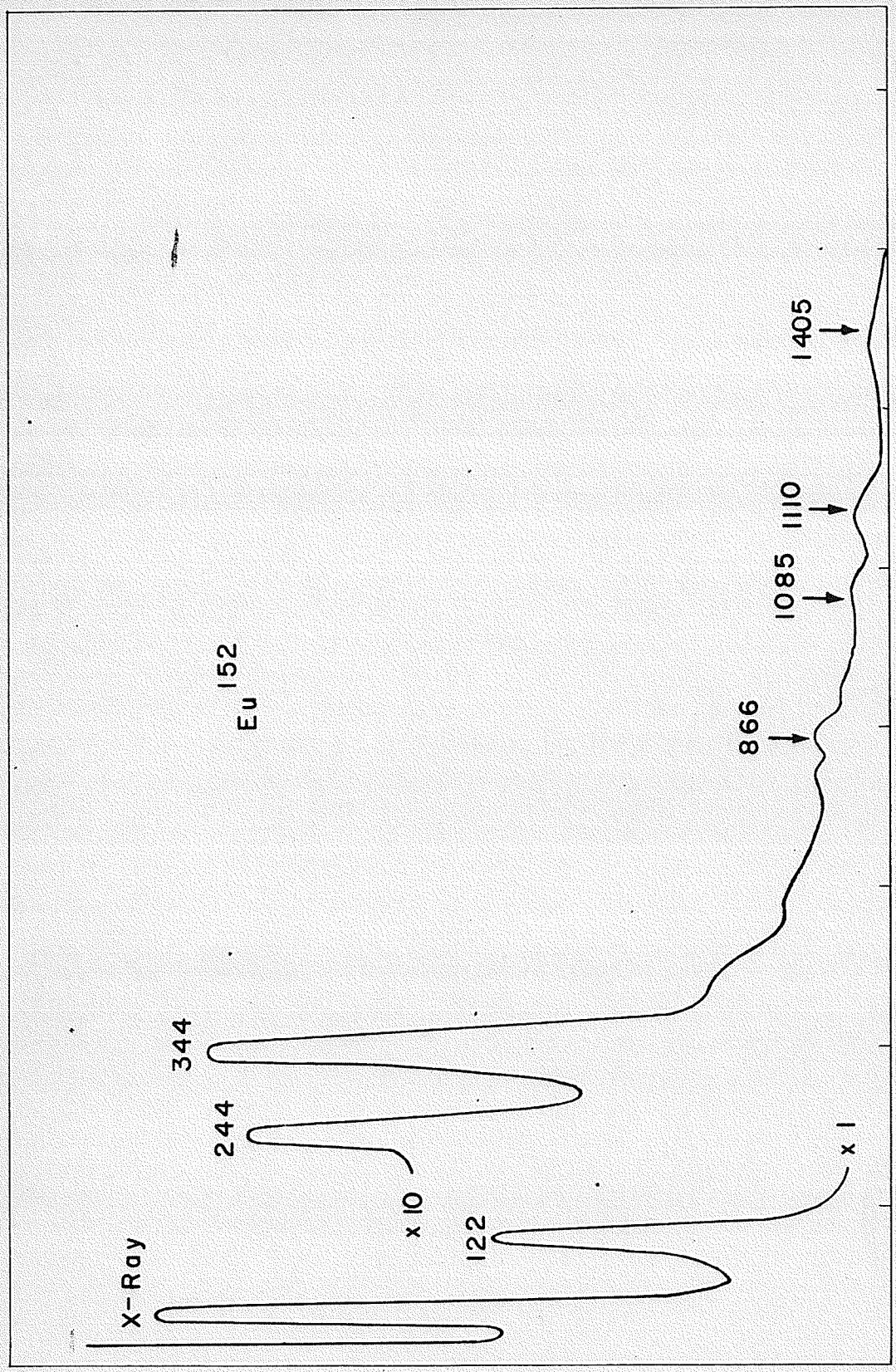

Fig. 15. Gamma-ray spectrum of $Eu^{152,154}$.

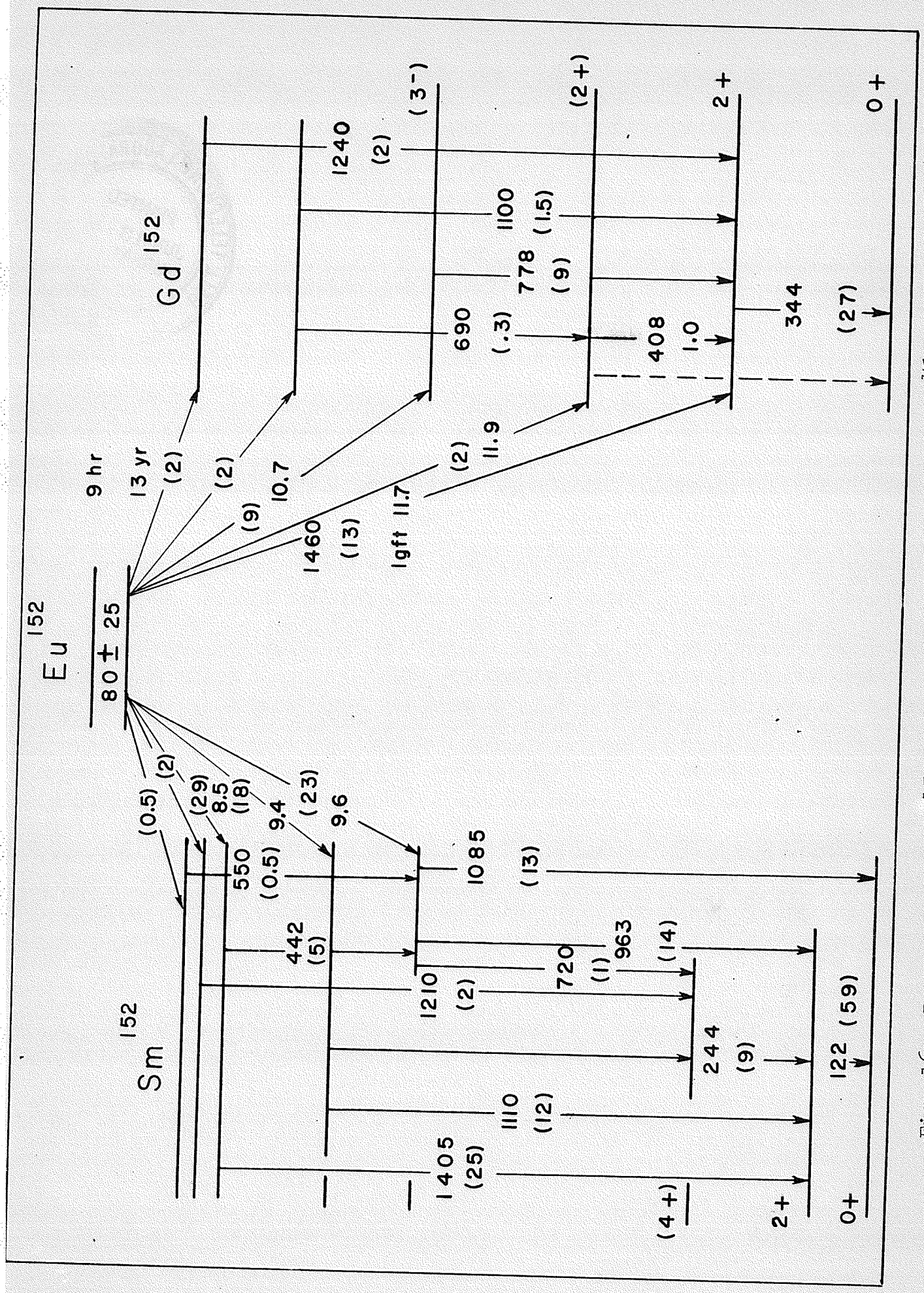

Fig. 16. Decay scheme of Eu^{152}. Courtesy of I.L. Grodzins (ZBP 64)

the decay percentages are in parentheses. The log FT values are on the K capture and beta branches.

There are several interesting angular correlation studied in the long-lived Eu^{152}, but only three will be discussed. There is the angular correlation of the 122 kev, 244 kev transition. Since $_{62}Sm^{152}$ is a strongly deformed nucleus one would expect the first and second excited states to be purely rotational levels with spins of 2+ and 4+ respectively. Coulomb excitation experiments (42) have shown that the spin of the 122 kev level is 2+. Internal conversion data place the spin of the 366 kev second excited state at 4+ but it is not conclusive (48). Thus it is desirable to perform an angular correlation experiment to determine the spin of the 366 kev level.

The second interesting correlation in Sm^{152} is that of the 1405 kev → 122 kev cascade. Because the 1527 kev level may be of high spin there is the possibility that its assignment could lead to the spin assignment of the ground state of Eu^{152}.

Unfortunately this experiment could not be performed because the 1405 kev line was so weak that the coincidence rate dropped to the level of the accidentals.

The third correlation is in Gd^{152}. The 408 → 344 kev cascade is very important because, from the point of view of the collective model, if one could measure the spin of the 752 kev level it will be the first time that the second excited state of a vibrational band near the transition region has been

definitely established. Unfortunately the 408 kev transition was so weak it could not be resolved, thus eliminating this very important correlation as a possible experiment. The only possible correlation that could be studied out of these three important cascades was the 244 → 122 kev cascade.

(ii) Procedure

Both lines of the 244 → 122 kev cascade were sufficiently intense due to the activity of Sm^{152} that they could be resolved. Further, since their pulse height ratio is 2 to 1 the three channel fast-slow coincidence spectrometer could be used to study it. Fischer and Marshall (20) found that the 6BN6 can be brought into current by pulses of different amplitude, i.e. a pulse of 2 volts would cause the 6BN6 to conduct if applied to G_1 but would not if applied to G_3. Thus a larger pulse would have to be applied to G_3 than to G_1. The bias was set so that the 6BN6 would conduct with a 122 kev pulse (3 volts) applied to G_1 and a 4 volt pulse on G_3. This provided satisfactory operation for the 244 → 122 kev cascade. The counting procedure was the same as that used on Ni^{60} with the fast-slow coincidence spectrometer. The coincidence counting rate for the 244 → 122 kev cascade was 35 every five minutes of which 1 was accidental.

(iii) Spin and Multipolarity Assignments

The spin of the 122 kev level will be taken as 2, a measurement obtained by coulomb excitation experiments (44). Since Sm^{152} is an even-even nucleus it has spin zero in the

ground state, hence the selection rule (3.2) states that the 122 kev gamma must be quadrupole. Thus the 244 → 122 kev cascade will be described by a spin sequence of the type $j_1(L_1)2(2)0$. Table VIII shows there are seven spin sequences of the $j_1(L_1)2(2)0$ type with the assumption that the 244 kev gamma-ray is either dipole or quadrupole. The seven spin sequences were obtained by applying selection rule (3.1). The theoretical values of the angular correlation coefficients along with the anisotropies are located in the appropriate columns in Table VIII.

Table VIII

Theoretical Values of Coefficients and Anisotropy			
Spin Sequence	A_2	A_4	A
1(1)2(2)0	-0.2505	0	-0.3339
2(1)2(2)0	+0.250	0	+0.4286
3(1)2(2)0	-0.0714	0	-0.1035
1(2)2(2)0	+0.1788	0	+0.2945
2(2)2(2)0	-0.0766	+0.326	+0.0766
3(2)2(2)0	-0.202	-0.0816	-0.3310
4(2)2(2)0	+0.102	+0.0091	+0.1667

Measured Values of Coefficients and Anisotropy								
Uncorrected				Corrected				
a_2'	A_2'	a_4'	A_4'	a_2	A_2	a_4	A_4	A
0.1133	0.0878	0.0282	0.0072	0.125	0.099	0.0416	0.0089	0.161

The experimental (measured) coefficients were obtained from a least squares fit of the data. Inspection of Table VIII shows that the measured coefficients and anistropy agree with the spin sequence 4(2)2(2)0. The error in the measured anisotropy is approximately 3%, which is not as good as the 1.2% error obtained with Ni^{60}. This agreement between theory and experiment lead the author to assign spin 4 to the 366 kev second excited state in Sm^{152} and a multipolarity of 2 to the 244 kev gamma. Thus, the spin sequence describing the 244 → 122 kev transition is $4(E_2)2(E_2)0$ with an angular correlation function given by:

$$W(\theta)-1 = +(0.099\pm0.006)P_2(\cos\theta) + (0.0089\pm0.004)P_4(\cos\theta). \qquad (3.10)$$

The assignment of spin 4 to the 366 kev second excited state means that the ground, first and second excited states in Sm^{152} are rotational states as predicted by the collective model of the nucleus. Figure 17 shows a plot of the corrected and uncorrected least squares fit to the experimental points for the $4(E_2)2(E_2)0$ assignment.

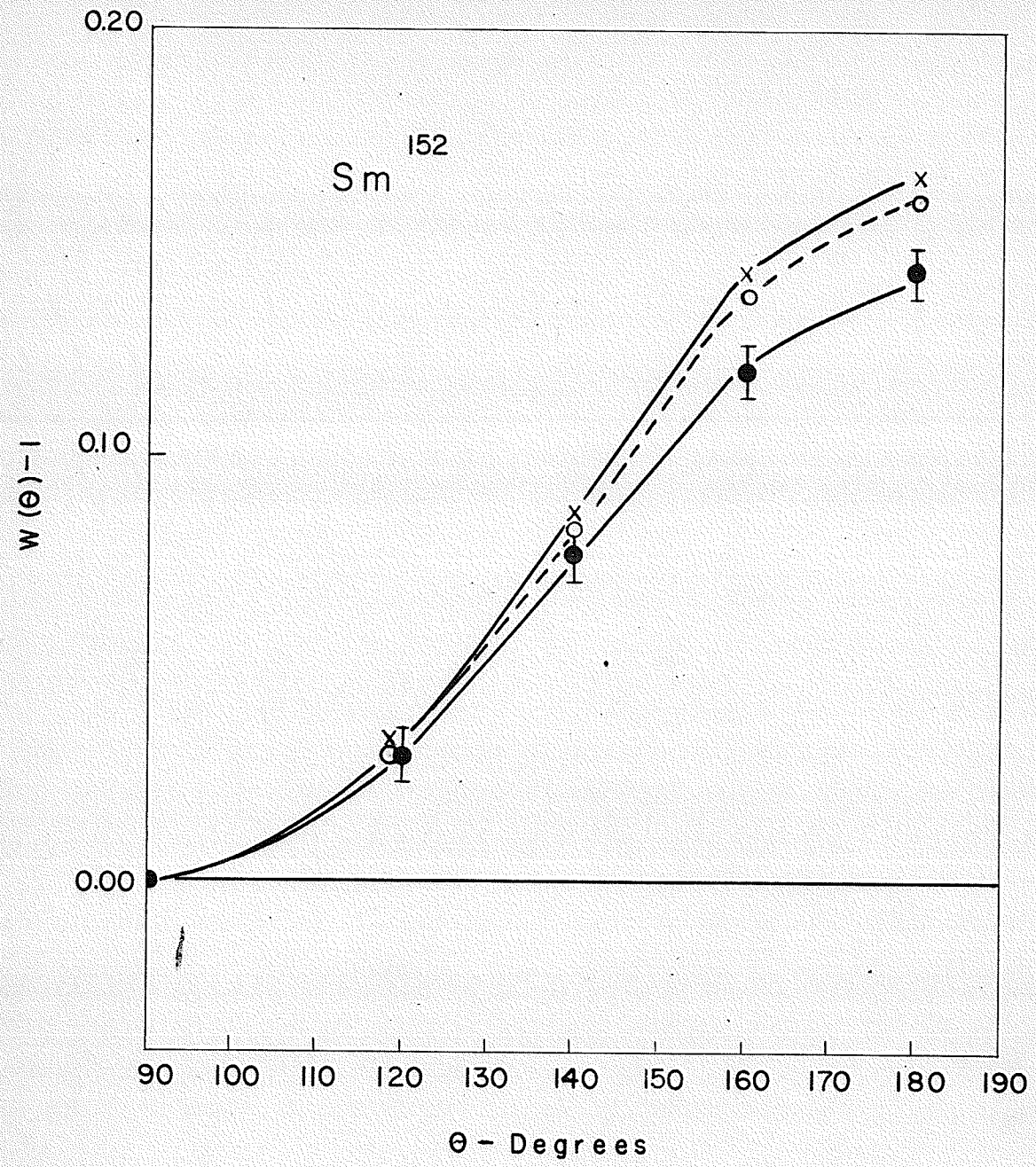

Fig. 17. Directional correlation curves for the 244 → 122 kev gamma-ray cascade in Sm^{152} obtained with the fast system. The lowest curve is $W(\theta)-1=0.0878P_2(\cos\theta)+0.0062P_4(\cos\theta)$: The least squares fit to the experimental points (black dots). The dashed curve with white dots is $W(\theta)-1=0.99P_2(\cos\theta)+0.0089P_4(\cos\theta)$: The least square fit corrected for finite angular resolution. The crosses are the theoretical points for a $4(E_2)2(E_2)0$ assignment.

(d) Directional Correlation in Ta^{181}

(i) Properties of Ta^{181}

Hf^{181} has a Z of 72 and a half life of 46 days. It decays by beta-minus emission to Ta^{181}. Ta^{181} contains five well-known gamma-rays, four of which are in triple and double cascade. Ta^{181}, with a Z of 73 is a strongly deformed nucleus but of the odd-A type. It has been studied by many investigators; McGowan in particular has studied both its beta-decay (55) and the angular correlation of its gamma-rays (56). Fan (57) has concluded that all of the gamma-ray transitions were pure multipoles on the basis of internal conversion coefficients obtained from electron intensity measurements. His results are in partial agreement with those of this investigation. H. Paul (58) of Purdue University has also studied the angular correlation of the gamma-rays in Ta^{181}.

The source was obtained from the Atomic Energy of Canada Limited with an activity of 20 microcuries. The target material was 10 milligrams of HfO_2 powder sealed in an aluminum tube 1/2" by 1/8". Figure 18 shows the bulk spectrum of Ta^{181} as obtained with spectrometer No. 2. The 132 kev-135 kev peak is composite while the peaks at 345 and 480 stand prominently displayed. The prominence of these cascade gamma-rays make it ideal for a correlation study. The decay scheme of Ta^{181} with the spin assignments of the excited states and the character of the gamma-rays is shown in Figure 19. This is taken from McGowan (56). The reason why Ta^{181} was chosen for study is that the

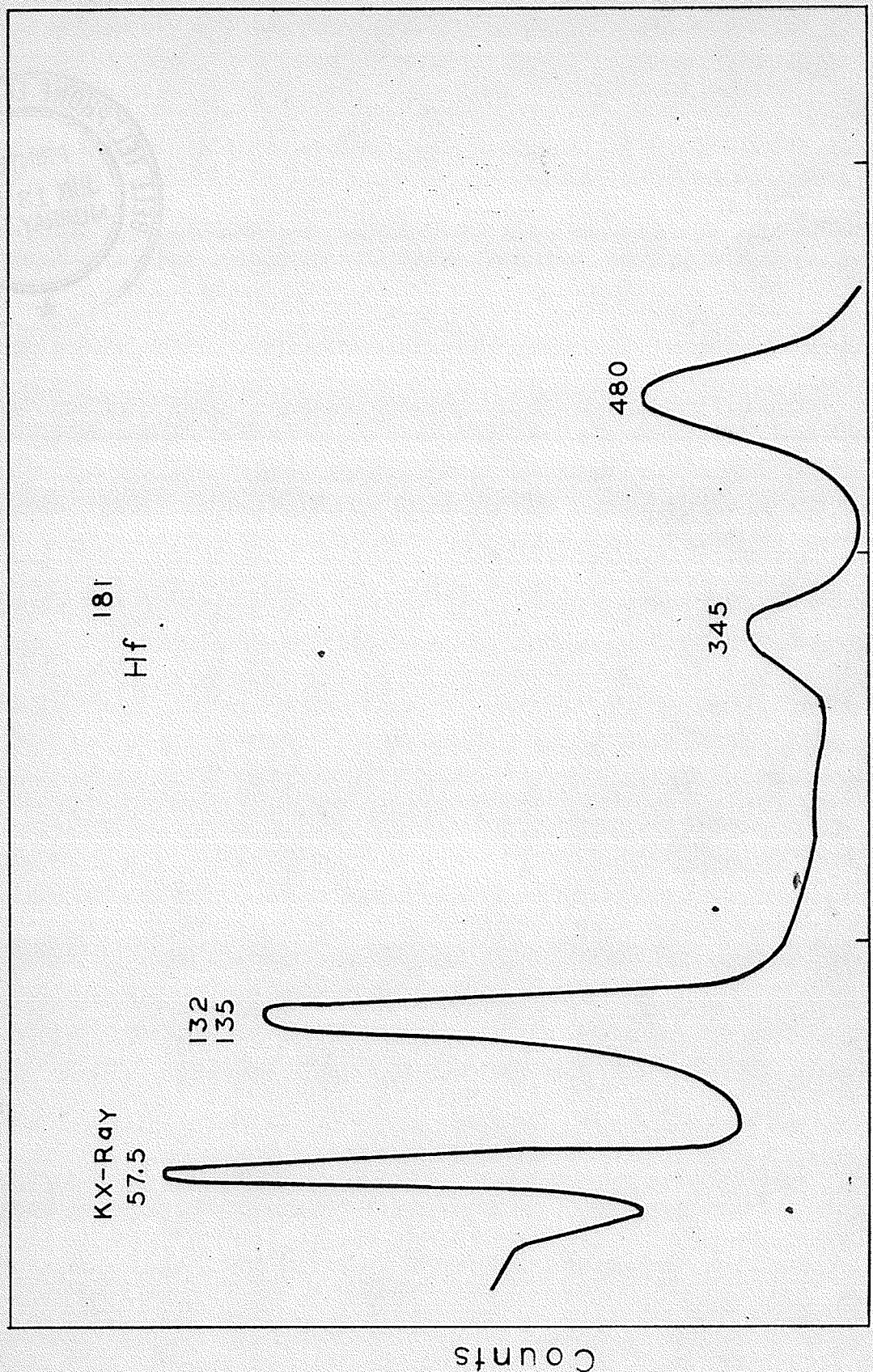

Fig. 18. Gamma-ray spectrum of Ta^{181} following beta-minus emission in Hf^{181}.

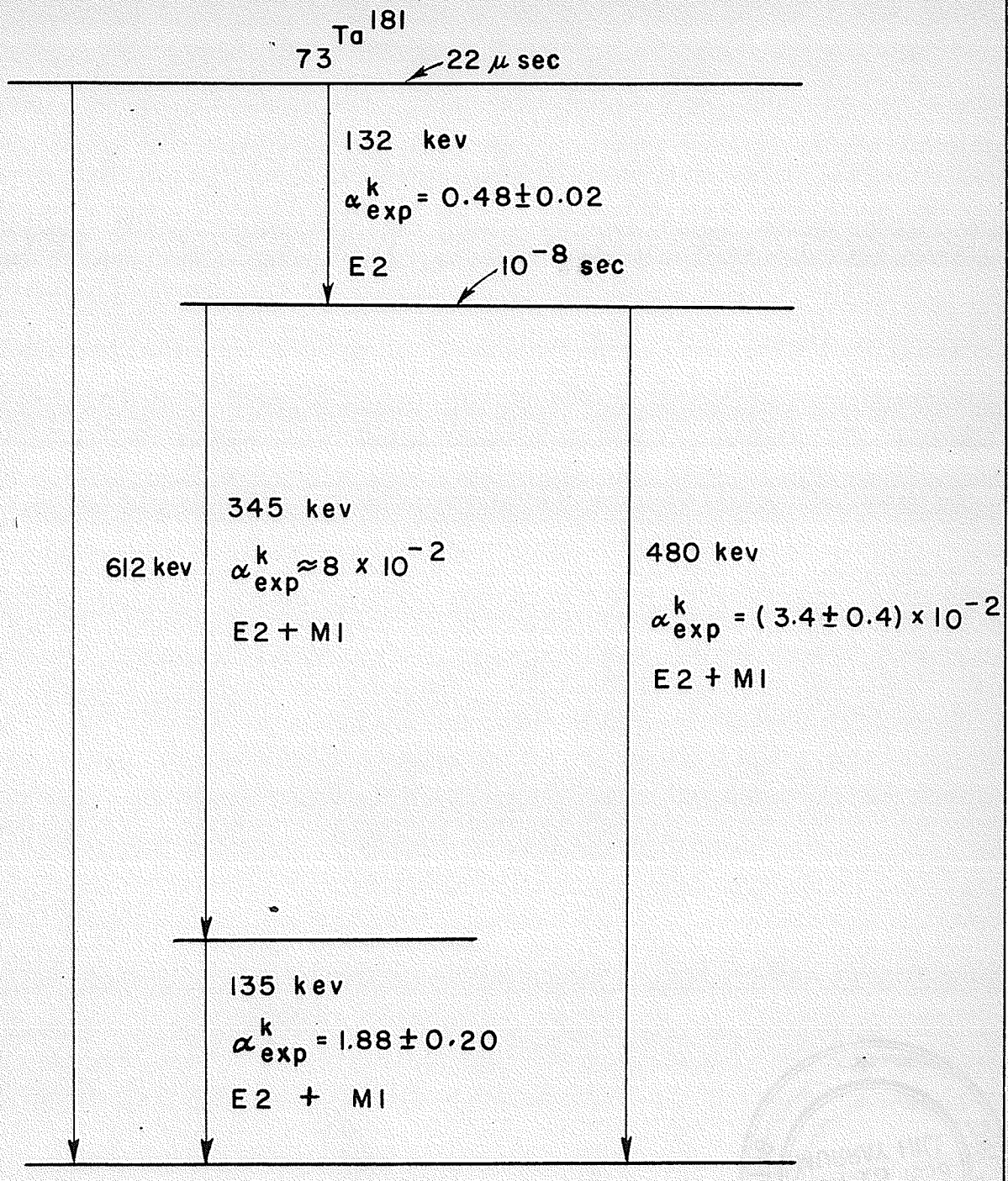

Fig. 19. Decay Scheme of Ta^{181}. After McGowan (56)

results of McGowan (56) and Paul (58) are at variance. Paul's results are as follows:

Gamma-ray Energy (Mev)	E_2	M_1
0.132	100%	
0.135	20%	80%
0.345	100%	
0.480	97%	3%

For the 0.132 Mev → 0.480 Mev cascade: 1/2 → 5/2 → 7/2.

For the 0.345 Mev → 0.135 Mev cascade: 5/2 → 9/2 → 7/2.

McGowan's results are as follows:

Gamma-ray Energy (Mev)	E_2	M_1
0.132	100%	
0.135	20%	80%
0.345	50%	50%
0.480	60%	40%

For the 0.132 Mev → 0.480 cascade: 5/2 → 9/2 → 7/2.

For the 0.345 Mev → 0.135 Mev cascade: 9/2 → 9/2 → 7/2.

They agree on the spins of the ground and first excited states, but disagree on the spins of the third and fourth excited states. The multipolarities of the 0.345 Mev transition and the 0.480 Mev transition are also in disagreement.

It was decided that rather than repeat the correlation of the 0.132 → 480 Mev correlation to determine the spins of the 480 kev level and the 612 kev level, it would be wiser to perform a separate correlation like the 132 → 345 kev correlation to see what the spins of these two top most levels would be.

This is by far a much more difficult correlation to perform than the 132 → 480 kev correlation.

Both Paul and McGowan agree that the 480 kev transition is of mixed multipolarity even though they disagree on the percentage of mixing. Meanwhile Paul states that the 345 kev transition is of pure multipolarity in agreement with Fan (47) while McGowan claims it is mixed. If the 345 kev line is pure then the 132 → 345 kev cascade will be a pure multipole correlation and its anisotropy and correlation coefficients will give an unambiguous spin assignment. Since the 480 kev line is undoubtedly mixed, the 132 → 480 kev correlation will give an anisotropy and correlation coefficients that are dependent on δ, the mixing ratio, and will yield an ambiguous result that can only be resolved by using internal conversion data. Since some of the internal conversion data is unreliable it was decided to perform the 132 → 345 kev correlation because of the possibilities of a spin assignment that could be determined wholly by angular correlation.

(ii) Procedure

The slow system was used with a resolving time of $\tau = 10^{-7}$ seconds because the pulse-height ratio was 2.6 to 1. The fast-coincidence unit works satisfactorily for pulse-height ratios less than 2 to 1. The same counting procedure was repeated here as with all other correlations; viz. six readings per position at 40 minutes per reading. The mean of these six readings was taken as the true reading. The gate of discriminator

No. 1 was set on the 132 kev peak while discriminator No. 2 was set on the 345 kev peak. Since the 135 kev line is also in cascade with the 345 kev line the net coincidence rate would be the sum of the coincidence rate due to the 132 kev → 345 kev cascade and the 345 → 135 kev cascade if no precautions were taken to eliminate the latter. Precautions were taken as follows: the 480 kev level has a mean lifetime of 10^{-8} seconds while the 135 kev level has a lifetime of less than 10^{-10} seconds. Since the 345 → 135 kev cascade is a prompt cascade (58), there is an average delay of 10^{-8} seconds between the emission of the 132 kev line and the 345 kev line while there is a delay of less than 10^{-10} seconds between the emission of the 345 kev line and the 135 kev line. Hence if a delay of 10^{-8} seconds is inserted into channel 1, which accepts the photopeaks due to the composite 132-135 kev line, the 132 → 345 kev cascade will be in coincidence while the 345 → 135 kev cascade will not since it is a prompt coincidence. An additional delay will exist between the 132 and the 345 kev lines due to their pulse heights. This was established by a fast oscilloscope and found to be of the order of 4×10^{-8} seconds or 0.04 microseconds. This was due to the slowness of the linear amplifiers used. The pulses due to the 345 kev line reached the lowest level of the gate of their differential discriminator 4×10^{-8} seconds after the pulses due to the 132 kev line reached the lowest level of the gate of their discriminator. Thus a total delay of 5×10^{-8} seconds existed between the two channels and a delay of 0.05 microseconds

was inserted into channel 1. It was found that the coincidence rate with zero delay in channel 1 was much higher than it was with the 0.05 microsecond delay, as would be expected since there are coincidences being counted that are also due to the prompt 345 → 135 kev cascade. The coincidence ratio for the 132 → 345 kev cascade using the 0.05 microsecond delay was 7 to 1.

With the photomultiplier voltage adjusted so that no blocking took place in either channel it was found that the pulse-height ratio was 2.6 to 1. When the photomultiplier voltage in channel 2 was raised to obtain a pulse height ratio of 1:1 blocking occurred for the 480 kev line. This prohibited the use of the fast coincidence circuit since its basis of operation relies on the fact that the whole spectrum must be in coincidence.

(iii) Spin and Multipolarity Assignments

The object of performing the 132 kev → 345 kev correlation was to determine the spins of the 480 kev level and the 612 kev level. Paul and McGowan agree on a spin of 9/2 for the first excited state. Further, they also agree along with Fan (57) that the 132 kev gamma-ray is pure E_2. Both Fan and Paul agree that the 345 kev gamma is pure electric quadrupole but McGowan claims it is 50% E_2 and 50% M_1. It was assumed, in view of the experimental evidence, that the first excited state has a spin of 9/2 and that both the 132 kev and the 345 kev gamma-rays were pure E_2. With these assumptions the 132 → 345 kev

cascade could be described by a spin sequence of the type $j_1(2)j(2)9/2$. The selection rules (3.1) and (3.2) allow 15 spin sequences of the type $j_1(2)j(2)9/2$. The theoretical values of the coefficients A_2 and A_4 for these sequences are shown in Table IX. The measured values of the coefficients were obtained from a least squares fit to the experimental points.

The spin sequence whose theoretical coefficients agree with the measured ones will be taken as the sequence that describes the 132 → 345 kev cascade. It will be noticed that both the measured coefficients are positive in sign. Thus, of the fifteen allowed spin sequences eleven are ruled out because of differences in sign leaving four possible spin sequences. Of these four the only sequence whose theoretical coefficients agree with the measured ones within the experimental error are those belonging to the spin sequence 1/2(2)5/2(2)9/2. This agreement led the author to assign a spin sequence of 1/2(2)5/2(2)9/2 to the 132 → 345 kev cascade. It is in diagreement with McGowan's assignments and multipolarity (56). Since this thesis was first submitted in August, 1956, McGowan has published a paper on polarization of gamma-rays in Ta^{181} (62) where he shows that his original assignment in (56) was in error and that the spins of the 612 kev and 480 kev levels are indeed 1/2 and 5/2 in agreement with the author's and Paul's results.

Figure 20 shows a plot of the uncorrected and corrected least squares fit to the experimental points for the 1/2(2)5/2(2)9/2 assignments. Table X shows the corrected and

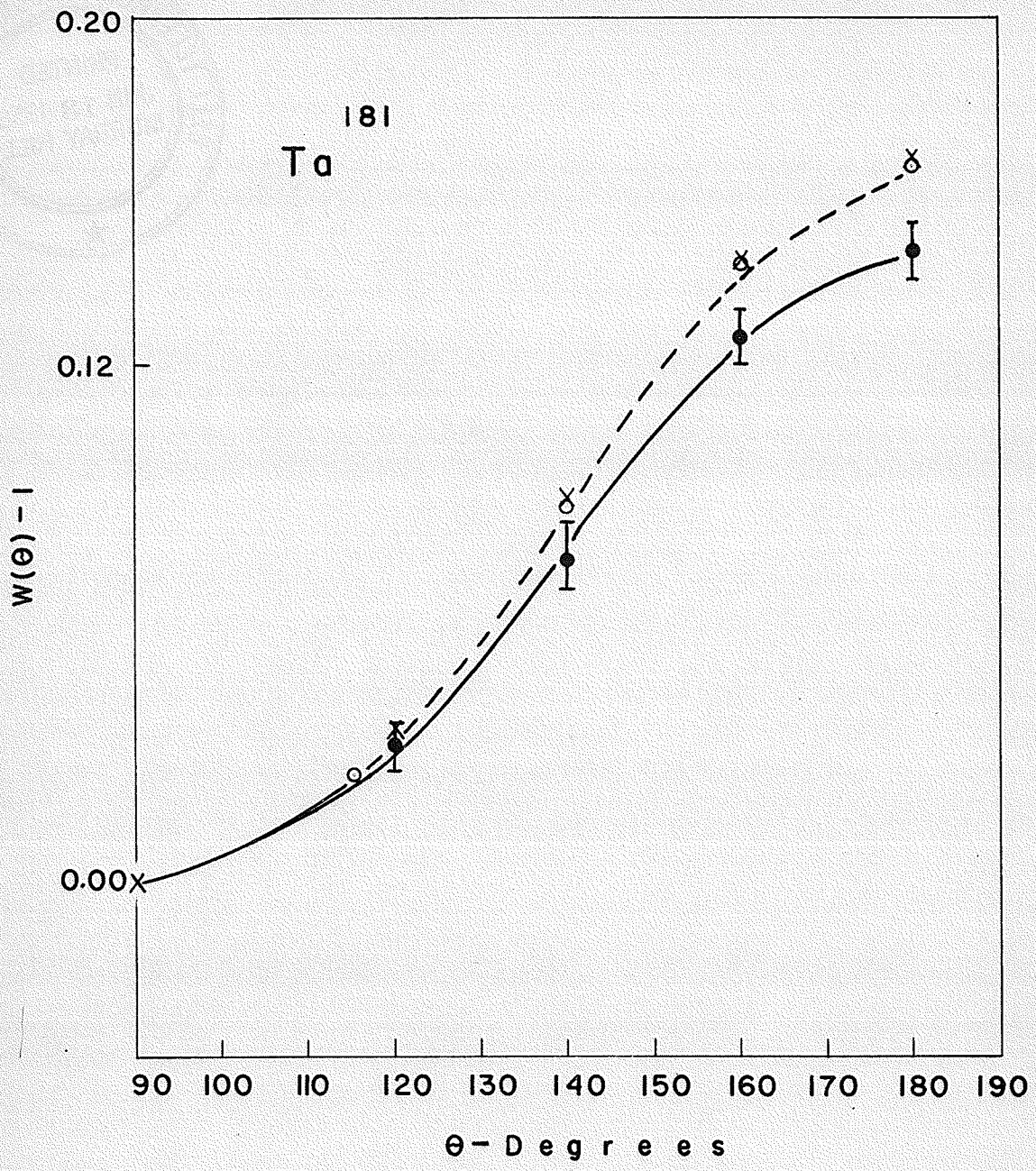

Fig. 20. Directional correlation curves for the 132 → 345 kev gamma ray cascade in Ta^{181} obtained with the slow system. The full curve is $W(\theta)-1=0.0895P_2(\cos\theta)+0.0063P_4(\cos\theta)$: The least squares fit to the experimental points (black dots). The dashed curve with white dots is $W(\theta)-1=0.101P_2(\cos\theta)+0.0091P_4(\cos\theta)$: The least squares fit corrected for finite angular resolution. The crosses are the theoretical points for a $1/2(E_2)5/2(E_2)9/2$ assignment.

uncorrected values of the angular correlation coefficients. Figure 21 shows the level scheme as predicted by the collective model of the nucleus for odd A. The notation is the same as that used in Fig. 14. The reactions appear to populate states belonging to three different rotational bands. Notice that the 612 kev level belongs to the third rotational band, the 480 kev level to the second and the 136 kev level to the first. The 132 kev → 345 kev cascade connects all three of the rotational bands in Ta^{181} and it can be readily understood why it could lead to confusion. The collective model also predicts that the transition (7/2, 9/2+) to (7/2, 7/2+) should have an E_2 intensity of 10 to 20% in agreement with both McGowan and Paul. The 303 kev level has not been observed but has become evident from coulomb excitation experiments (57).

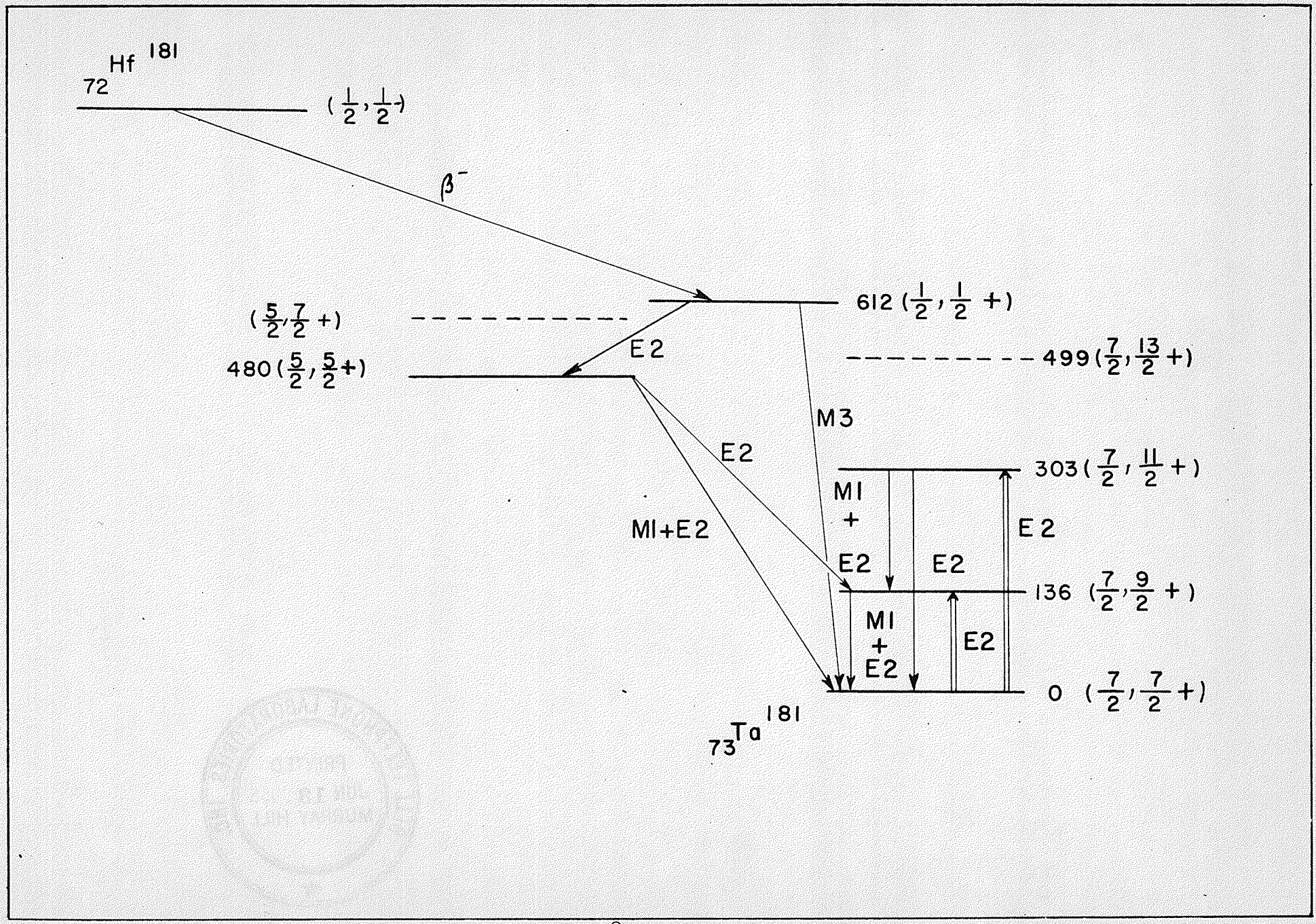

Fig. 21. Level scheme of Ta^{181} as predicted by the collective model of the nucleus. After Alaga et al (53).

Table IX

Theoretical Values of Coefficients

Spin Sequence	A_2	A_4
1/2(2)5/2(2)9/2	0.102	0.0091
3/2(2)5/2(2)9/2	0.0364	-0.0104
5/2(2)5/2(2)9/2	-0.0364	0.0058
7/2(2)5/2(2)9/2	-0.062	-0.0017
9/2(2)5/2(2)9/2	0.0364	0.0002
3/2(2)7/2(2)9/2	-0.1387	-0.0621
5/2(2)7/2(2)9/2	-0.0231	0.111
7/2(2)7/2(2)9/2	0.074	-0.083
9/2(2)7/2(2)9/2	0.0878	0.0301
11/2(2)7/2(2)9/2	-0.0646	-0.0044
5/2(2)9/2(2)9/2	-0.119	0.1378
7/2(2)9/2(2)9/2	-0.0542	-0.305
9/2(2)9/2(2)9/2	0.0756	0.263
11/2(2)9/2(2)9/2	0.0756	-0.108
13/2(2)9/2(2)9/2	-0.065	0.0173

Measured Values of Coefficients

	A_2	A_4
Corrected	0.101 ± 0.002	0.0091 ± 0.001

Table X

Angular Correlation Coefficients for the 132 → 345 kev Cascade in Ta^{181}

Uncorrected				Corrected			
a_2'	A_2'	a_4'	A_4'	a_2	A_2	a_4	A_4
0.116	0.0895	0.029	0.0063	0.1232	0.101	0.0418	0.0091

Chapter IV

Summary and Conclusions

A fast-slow coincidence spectrometer has been developed and applied to the directional correlation of Ni^{60} and Sm^{152}. The fast coincidence unit was a 6BN6 Fischer and Marshall (26) type unit which was operated at a resolving time of 2×10^{-8} seconds. Due to the absence of pulse shaping circuits in the fast channel the fast-slow spectrometer could only study those gamma-ray cascades that have a pulse-height ratio of 2 to 1. The 1172 → 1332 kev cascade in Ni^{60} was such a cascade along with the 244 → 122 kev cascade in Sm^{152}. Since the Ni^{60} cascade is considered a "standard" in directional correlation work the study of this cascade also calibrated the fast-slow spectrometer for the study of the 244 → 122 kev cascade in Sm^{152}.

The two-channel coincidence spectrometer was used to study W^{182} and Ta^{181}. The innovation of a Sorenson regulator and a Hamner high-voltage supply stabilized the equipment so that a given photoelectron line drifted by a tenth of one percent per twenty-four hour period, thus making the study of a complicated isotope like W^{182} possible.

The isotopes that were studied were chosen to test the theory of the collective model of the nucleus as put forward by Bohr and Mottelson. ${}_{72}W^{182}$, ${}_{62}Sm^{152}$ and ${}_{73}Ta^{181}$ all have atomic numbers that lie in the range $60 \leq Z \leq 92$ which is called the

"strong coupling region." Nuclei that have a Z in this region are called "strongly deformed nuclei." Their gamma-ray spectra are characterized by rotational levels that are disturbed due to the strong deformations caused by nucleons outside of closed shells. These deformations can be characterized by K-forbiddenness which can give rise to a multiplicity of rotational bands in a given spectrum.

The study of cascades which connect these rotational bands would provide a test of the theory. The 67.4 → 1222 kev cascade in W^{182} gave a correlation which satisfied a 2 → 2 → 0 assignment. If W^{182} was characterized by one rotational band this would have to be a 12 → 8 → 0 assignment. This established that W^{182} possessed more than one rotational band. The collective model states that the 67.74 transition is a transition between the first state of the third band and the first state of the second band. The 1222 kev line is a transition from the first state of the second band to ground. The collective model assigns a spin sequence of 2 → 2 → 0 to this cascade in agreement with experiment.

Similarly the 152.4 → 1222 kev is another such cascade where the 152.4 transition occurs between the second state of the third band and the first state of the second band. The experimentally determined assignment was 3 → 2 → 0 for 152.4 → 1222 kev cascade, which agrees with the collective model of the nucleus. Another feature of this model is that it predicts a very high percentage of E_2 in the transitions between the second and first

rotational bands. The 67.4 → 1122 kev cascade is one where the 67.4 transition is between the third and second band while the 1122 kev transition occurs between the second and first. The directional correlation measurement of this cascade yielded the assignment $2(E_1) \rightarrow 2(90\%\ E_2,\ 10\%\ M_1) \rightarrow 2$. The high percentage of E_2 in the 1122 kev transition agrees with the collective model and internal conversion data. Thus the experimental results verify the predictions of the collective model in that W^{182} contains at least three rotational bands with the transitions between the second and first band being primarily E_2 because M_1 is K-forbidden. $_{62}Sm^{152}$ is an even-even nucleus which should have $j = 2$ for the first rotational band with spin zero for the ground state. The directional correlation studied in Sm^{152} was the 244 → 122 kev cascade which connects the second, first and ground states. The experimentally determined assignment was $4 \rightarrow 2 \rightarrow 0$ in agreement with the collective model.

Ta^{181} is a much studied isotope but there are conflicting spin assignments on the two topmost levels.[56,58] A correlation was selected that would provide an unambiguous assignment of these upper levels. The 132 → 345 kev cascade would provide such an assignment if each transition was pure E_2. The assumption was that if they were pure they would be independent of the mixing ratio δ and hence the accuracy of the measurement would not have to rely on internal conversion data for an unambiguous assignment. The measured correlation indicated an assignment of $1/2 \rightarrow 5/2 \rightarrow 9/2$ with multipolarity pure E_2 for each transition.

This assignment also agreed with the collective model, which states that this cascade occurs between the third, second and first rotational bands. The levels in these bands that are connected by 132 → 345 kev cascade have spins of 1/2, 5/2 and 9/2 respectively.

The conclusions are that the collective model of the nucleus provides an adequate description of nuclei with a $60 \leq Z \leq 92$ and that directional correlation studies are a valuable tool in studying the predictions of this model. The fast-slow coincidence spectrometer is a high precision spectrometer capable of measuring correlations to within one percent.

ACKNOWLEDGEMENTS

The author wishes to thank Dr. K. I. Roulston for his advice during the final stages of this thesis. Dr. S. Standil and Dr. R. W. Pringle are also to be thanked for their many interesting conversations on the earlier stages of the work.

REFERENCES

(1) H. Kallman, Natur and Technik, July, 1947.

(2) E. L. Brady and M. Deutsch, Phys. Rev. 74 (1948) 1541.

(3) D. R. Hamilton, Phys. Rev. 58 (1940) 122.

(4) L. C. Biedenharn and M. E. Rose, Rev. Modern Physics, 25 (1953) 729.

(5) L. C. Biedenharn, G. B. Arfken and M. E. Rose, Phys. Rev. 83 (1951) 586.

(6) G. B. Arfken, L. C. Biedenharn and M. E. Rose, Phys. Rev. 86 (1952) 761.

(7) J. Weneser and D. R. Hamilton, Phys. Rev. 92 (1953) 321.

(8) E. J. Hellund and J. M. Jauch, Phys. Rev. 92 (1953) 203.

(9) M. Walter, O. Huber and W. Zunti, Helv. Phys. Acta. 23 (1950) 697.

(10) E. L. Brady and M. Deutsch, Phys. Rev. 78 (1950) 558

(11) M. E. Rose, Phys. Rev. 91 (1953) 610.

(12) J. S. Lawson and H. Frauenfelder, Phys. Rev. 91 (1953) 649.

(13) M. Walter, O. Huber and W. Zunti, Ibid.

(14) Annual Review of Nuclear Science (Annual Reviews, Inc.; Stanford 1953) Vol. 2 P148.

(15) S. Frankel Phys. Rev. 83 (1951) 673.

(16) S. Frankel, to be published in Phys. Rev.

(17) E. L. Church and J. J. Kraushaar Phys. Rev. 88 (1952) 419.

(18) M. E. Rose, to be published in the Phys. Rev.

(19) G. A. Morton, Nucleonics 10 (1952) 39.

(20) J. Fischer and J. Marshall, Rev. Sci. Instrum. 23 (1952) 47.

(21) K. Roulston, Nucleonics 7 (1950) 27.

(22) P. R. Bell, Scintillation Method, in Beta and Gamma-Ray Spectroscopy. Interscience Publishers, Inc. P 142.

(23) K. Roulston Ph.d. Thesis. University of Manitoba 1952

(24) H. W. Taylor Ph.d. Thesis. University of Manitoba 1954.

(25) H. W. Taylor, Ibid p.41.

(26) Z. Bay, Rev. of Sci. Instrum. 22 (1951) 397.

(27) Birks " Scintillation Counters" McGraw Hill Co. Ltd. Curran "Luminescence and the Scintillation Counter" Academic Press.

(28) H. W. Taylor, Ibid p. 66.

(29) Keister and Schmidt, Phys. Rev. 93 (1954) 140.

(30) Aeppli, Frauenfelder, Heer and Ruetsch, Phys. Rev. 87 (1952) 379.

(31) Klema and McGowan, Phys. Rev. 91 (1953) 616.

(32) Steffen, Beta and Gamma-Ray Spectroscopy, Interscience Publishers, Inc. P 553.

(33) Lloyd, S. P. Phys. Rev. 83 (1951) 716.

(34) Cork, Childs, Branyan, Rutledge and Stoddard Phys. Rev. 81 (1951) 642.

(35) Fowler et al, Phys. Rev. 94 (1954) 1082.

(36) Mihelich, J. W., Phys. Rev. 95 (1954) 626.

(37) Muller et al, Phys. Rev. 88 (1952) 775.

(38) Murray et al, Phys. Rev. 97 (1955) 1007.

(39) Rose, et al, Phys. Rev. 83 (1951) 79.

(40) Gellmann et al, Phys. Rev. 85 (1952) 944.

(41) Bohr, A. and Mottelson, B. Phys. Rev. 90 (1953) 717.

(42) McClelland et al, Phys. Rev. 93 (1954) 904.

(43) Temmer, G. M. and Heydenburg, N. P. Phys. Rev. 99 (1955) 609.

(44) Temmer, G. M. and Heydenburg, N. P. Phys. Rev. 99 (1955) 609.

(45) Huus, T. and Lunden, A., Phot. Mag. 45 (1954) 966.

(46) Taylor, H. W., Ibid Page 110.

(47) Alaga, G. et al, "Intensity rules for Beta and Gamma Transitions to rotational states." *Dan. Mat. Fys. Medd. 29, no 9 (1955)*

(48) Grodzins, I. L. Brookhaven National Laboratory, by private communication (July, 1956).

(49) Hill, J. M. and Shepherd, L. R. Proc. Phys. Soc. (London) A63 (1950) 126.

(50) Cork et al, Phys. Rev. 72 (1947) 1209; 73 (1948) 78.

(51) Shull, F. B. Phys. Rev. 74 (1948) 917.

(52) Cork et al, Phys. Rev. 77 (1950) 848.

(53) Shavtvalor, L., J. J. Expt. Theoret. Phys. (U.S.S.R.) 21 (1950) 1123.

(54) Slatterly et al, Phys. Rev. 96 (1954) 465.

(55) McGowan, F. K., Phys. Rev. 93 (1954) 163.

(56) McGowan, F. K., Phys. Rev. 93 (1954) 471.

(57) Fan, Chang-Yun, Phys. Rev. 87 (1952) 252.

(58) Paul, H., Purdue University. Dissertation. Nuclear Science Abstracts 15 (1955) 855.

(59) Heydenburg, N. P. and Temmer, G. M., Phys. Rev. 100 (1955) 150.

(60) S. P. Lloyd, Physical Review 83 (1951) 716.

(61) Siegbahn, K., Beta and Gamma-Ray Spectroscopy.
Interscience Publishers, Inc., Chapter XIX P 550.

(62) Stelson and McGowan, Physical Review 105 (1957) 1346.